



# Plant-derived silica nanoparticles and composites for biosensors, bioimaging, drug delivery and supercapacitors: a review

S. Prabha<sup>1</sup> · D. Durgalakshmi<sup>1</sup> · Saravanan Rajendran<sup>2</sup> · Eric Lichtfouse<sup>3,4</sup>

Received: 14 April 2020 / Accepted: 17 October 2020 / Published online: 12 November 2020  
© Springer Nature Switzerland AG 2020

## Abstract

Silica nanoparticles have rapidly found applications in medicine, supercapacitors, batteries, optical fibers and concrete materials, because silica nanoparticles have tunable physical, chemical, optical and mechanical properties. In most applications, high-purity silica comes from synthetic organic precursors, yet this approach could be costly, polluting and non-biocompatible. Alternatively, natural silica sources from biomass are often cheap and abundant, yet they contain impurities. Silica can be extracted from corn cob, coffee husk, rice husk, sugarcane bagasse and wheat husk wastes, which are often disposed of in rivers, lands and ponds. These wastes can be used to prepare homogenous silica nanoparticles. Here we review properties, preparation and applications of silica nanoparticles. Preparation includes chemical and biomass methods. Applications include biosensors, bioimaging, drug delivery and supercapacitors. In particular, to fight the COVID-19 pandemic, recent research has shown that silver nanocluster/silica deposited on a mask reduces SARS-Cov-2 infectivity to zero.

**Keywords** Silica nanoparticles · Structure · Biomass · Rice husk · Sugarcane bagasse · Corn cob · Synthesis · Applications · Theranostic · Supercapacitor

## Introduction

Silicon is a major element of earth's crust. Silica sand, the primary ore source of silicon, is abundant and easy to process. Silica minerals are referred by quartzite, tridymite, metamorphic rock, cristobalite and minerals such as polymorphs of silica. The combination of silicon and oxygen is called silicate, and 90% of earth's crust is made of silicate minerals. Clays and silica sand are silicate minerals that are used in applications such as making Portland cement in building mortar and modern stucco. Concrete made of silicates integrated within silica sand for making concrete is a major building material (Greenwood and Earnshaw 1997). Silicones are used for various products such as mold-release agents, molding compounds, waxes, waterproofing treatments, mechanical seals and high-temperature greases. Silica in the form of clay and sand is used in bricks and concrete. Glass silica obtained from sand is the major element in making various glass material with diverse properties. The silly putty contains also substantial amounts of silica, it is made by addition of boric acid to silicone oil. Liquid silicone is widely used as dry cleaning solvent and is an alternative for perchloro-ethylene solvents (Koch and Clément 2007).

---

✉ D. Durgalakshmi  
durgaklakshmi@gmail.com

S. Prabha  
spriyadharshni12@gmail.com

Saravanan Rajendran  
Saravanan3.raj@gmail.com

Eric Lichtfouse  
eric.lichtfouse@gmail.com

- <sup>1</sup> Department of Medical Physics, Anna University, Chennai 600025, India
- <sup>2</sup> Departamento de Ingeniería Mecánica, Facultad de Ingeniería, Universidad de Tarapacá, Avda. General Velásquez, 1775 Arica, Chile
- <sup>3</sup> Aix-Marseille Univ, CNRS, IRD, INRAE, Coll France, CEREGE, Avenue Louis Philibert, 13100 Aix en Provence, France
- <sup>4</sup> International Research Centre for Renewable Energy, State Key Laboratory of Multiphase Flow in Power Engineering, Xi'an Jiaotong University, Xi'an 710049, China

Silica is also used in biomedical applications such as contact lenses, breast implants, explosives and pyrotechnics.

Nanotechnology involves the development of nano-sized materials and devices. Notably, silica nanoparticles have occupied the prime position due to their facile synthesis, rich surface chemistry, low toxicity and controllable properties such as optoelectronic, mechanical and chemical stability (Rossi et al. 2005; Vivero-Escoto and Huang 2011). These properties are not only extensively considered in biomedical field and but also for diverse applications such as agricultural, food industries, photovoltaic and energy storage applications (Lieberman et al. 2014; Devi and Balachandran 2016). Nanotechnology enables the extension of multifunctional medicine by integrating materials that allow multimodal imaging and theranostics applications (Bharti et al. 2015). Notably, mesoporous silica nanoparticles have uniform pore size, hydrophilic surface property and high surface area. Such properties increase electrochemically active centers, thus enhancing electron transport and promoting electrolyte penetration, which meets the requirements of next-generation supercapacitors (Huang et al. 2013).

Silica nanoparticles have also been applied for fighting COVID-19. Here, a nanocomposite of silver nanocluster/silica deposited on a FFP3 mask reduces the SARS-Cov-2 to zero (Balagna et al. 2020). The nanocomposite also increases the life time of the mask and improves air filtering. Moreover, silica nanoparticles can be transformed to have a superhydrophilic surface which repels contaminated droplets (Meguid and Elzaabalawy 2020).

Natural resources-based silica has garnered considerable interest in the materials science and biomedicine fields owing to its low cost, eco-friendliness, bioactivity and availability. Biomass is an alternative source for widely used organic precursors, namely tetraethyl orthosilicate (TEOS) and tetramethylorthosilicate. In biomedical applications, stability and biocompatibility are the prime issues. Therefore research is focussing on the development of biomass for preparing silica and implemented to theranostics applications.

Developed countries have followed the concept by which waste materials are not really waste but new sources for creating new materials. Developing countries have abundant agriculture-based resources and their by-products are used to produce various low-value products. In 2005, a bioenergy production project using municipal, animal, agricultural and industrial wastes was assigned by five countries: India, China, Sri Lanka, Philippines and Thailand. As a result, in 2010, bioenergy represented 45% of total energy in India, 17% in China, 33% in Sri Lanka, 34% in Philippines and 14% in Thailand. India is the major energy consumer in Asia. During 2011, biomass gasifier assignment of 0.5 MW power in Tamil Nadu and 1.20 MW in Gujarat were successfully installed (Pode and Reviews 2016).

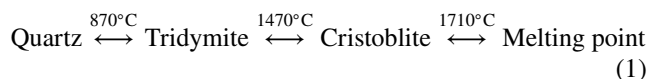
In India, 120 million tons of paddy rice is produced per annum, giving nearly 4.4 tons of rice husks (Giddel and Jivan 2007). High silica content has been observed in biomass wastes (Oladeji 2010; Shen et al. 2014; Zemnukhova et al. 2015; Hossain et al. 2018; Dhinasekaran et al. 2020). Rice husk ash contains 83–98% of silica (Saxena et al. 2009; Babaso and Sharanagouda 2017). Corn is another major crop plant with 785 million tons produced annually in this world. India is the seventh largest producer of corn cob, with silica content as high as 60% in biomass (Kumar et al. 2010). India produces an average of 500 million tons of crop residue per year, of which 140 million tons is surplus and 92 million tons is left as burned (Bhuvaneshwari et al. 2019). Globally, uncontrolled burning of biomass wastes is causing environmental and health issues, thus calling for recycling options.

Recent research on silica has focused on nanoparticles. Silica nanoparticles can be prepared from either organic chemicals or biomass. Comparatively, the usage of biomass is less compared to synthetic organic precursors due to lack of a review and assessment on the importance of silica in biomass. Many reports have reviewed the preparation of silica nanoparticles from pure organic chemicals (Wu et al. 2013a, b; Bleta et al. 2018; Morin-Crini et al. 2019; Meena et al. 2020; Mahajan et al. 2020). Here we focus on silica nanoparticles from biomass for biosensors, bioimaging, drug delivery and supercapacitor applications.

## Structural properties of silica minerals

### Crystalline and amorphous structure

Solid materials are generally crystalline, made of atoms, molecules and ions arranged in an orderly repeating pattern. In amorphous materials, atoms are not arranged in orderly repeating patterns. Silica has two types of structures: crystalline and amorphous. Silica occurs naturally as the solid amorphous phase of flint and opal and as the crystalline phase of cristobalite, quartz and tridymite. Amorphous phases can be transformed into crystalline phases by thermal treatments (Eq. (1)) (Waddell 2000).



Quartz and sandstone are the impure forms of silica. The crystalline phases of silica are melanophlogopite,  $\alpha$ -quartz,  $\alpha$ -cristobalite,  $\beta$ -quartz,  $\beta$ -cristobalite,  $\gamma$ -tridymite,  $\beta$ -tridymite,  $\alpha$ -tridymite, fassigite, chalcedon, keatite, moganite and stishovite. Amorphous phases of silica include hyalite opal, natural silica glass, sintered pearl, lechatelierite are amorphous phases of silica (Fanderlik 2013). There are three polymorphic structures present in the silica, each structure having both low-temperature ( $\alpha$ ) and a high-temperature

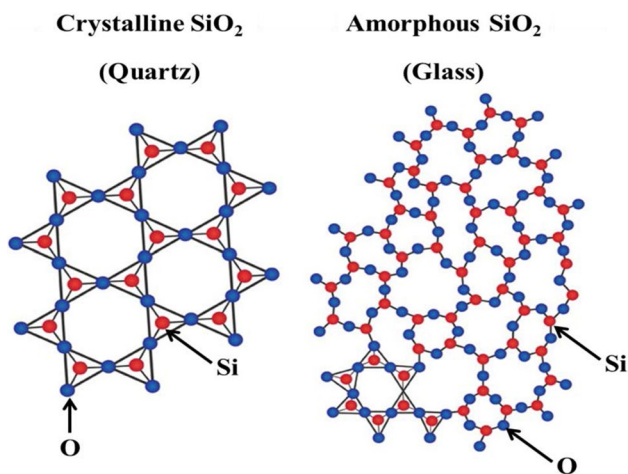


Fig. 1 Structure of crystalline and amorphous silica

( $\beta$ ) forms (Douglas and Ho 2006). In sediments, the transformation of amorphous silica opal-A into crystalline opal-CT (cristobalite-tridymite) with increasing burial, temperature and pressure has been correlated with an abrupt transformation of organic matter (Lichtfouse and Rullkötter 1994).

Figure 1 shows the structure of both crystalline and amorphous silica structures.

Silica and silicones

In 1800, Sir Humphry Davy thought that silica has to be a compound and not a single element. To test this hypothesis, in 1808 he did experiments to decompose of silex, alumine and glucine zircon, yet he failed to isolate the Si metal. In 1811, Louis-Jacques Thenard (1777–1857) and Louis-Joseph Gay-Lussac (1778–1850) explained that heating potassium with silicon tetrafluoride results in the formation of impure amorphous silicon. Silicon was discovered by Jakob Berzelius (1779–1848); in 1824, he prepared amorphous silicon successfully using earlier methods, and then, he removed fluorosilicates by repeated washing to get the purified product. The name silica is coming from the Latin word *silex*. Silica is the combination of silicon (Si) with oxygen ( $O_2$ ) and the most plentiful compound in the earth’s crust (Pauling 1957; Holden 2001). The covalent network structure of  $SiO_2$  is given in Fig. 2.

Among all polymers, organic groups attached to a chain of inorganic atoms is a unique properties of silicone. Silicones are used in of electronics, paints, construction and beverages (Korzhinsky et al. 1995). In medicine, silicone is used in artificial joints, antacids, implants of various notoriety and pacemakers (Korzhinsky et al. 1995). Silicon dioxide (silica) occurs in the form of sand. Reduction of silica with carbon at high temperature was performed for manufacturing

Fig. 2 Possible covalent network structure of silica— $SiO_2$

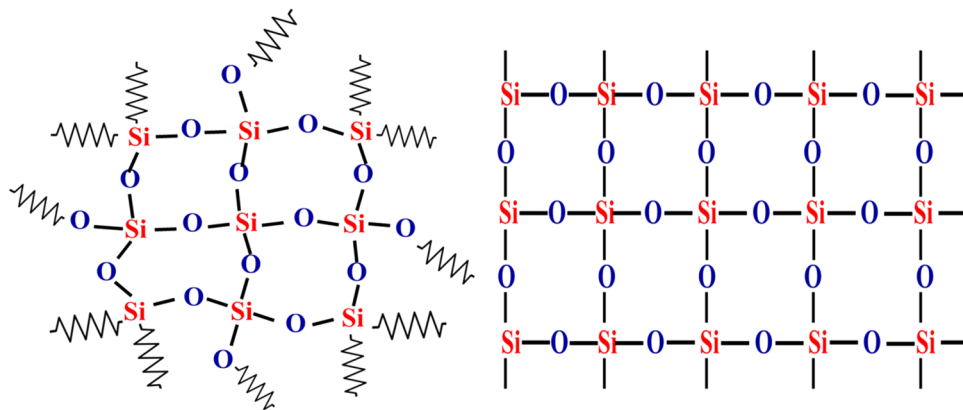
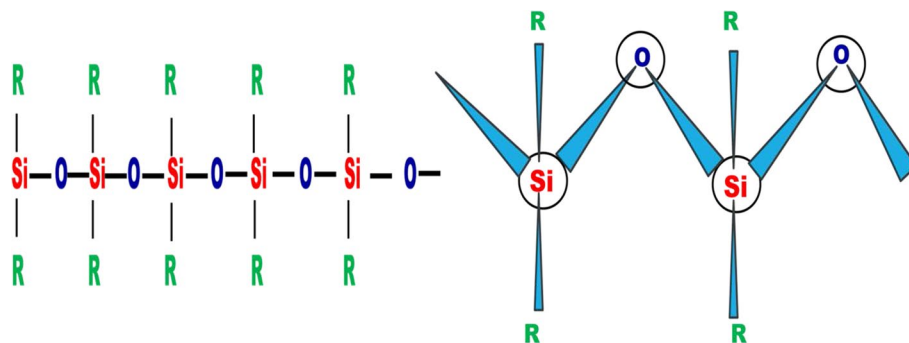
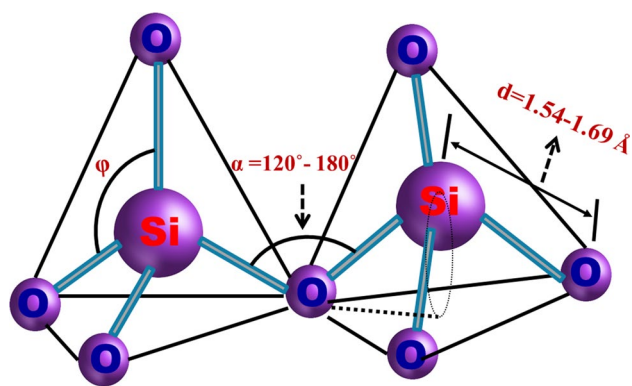


Fig. 3 Molecular structural arrangements of silicones





**Fig. 4** 3D schematic of the regular silica structure. Modified after Salh (2011)

silicone (Eq. (2), Bell et al. 1968; Mozzi and Warren 1969; Gerber and Himmel 1986; Korzhinsky et al. 1995).



The  $\text{SiO}_4$  tetrahedron is the central functional component of both amorphous and crystalline of silica. The silicon

atom is placed at the center, and the four oxygen atoms are connected at each side of a tetrahedron (Fig. 3, Henderson and Baker 2002). According to various forms of silica, the tetrahedron depends on the angle ( $\alpha$ ) and bond length.

The energy of the Si–O bond is 4.5 eV (Devine et al. 2000). Figure 4 shows the 3D silica structural parameters of bond length ( $d$ ), polyhedron angle ( $\phi$ ) and inter-tetrahedral bond angle ( $\alpha$ ) (Lide 2004).

In Raman spectra, bands correspond to  $\text{Si-O}^-$  groups of various  $Q^n$  units ( $n < 4$ ). The band at 1050–1100  $\text{cm}^{-1}$  is due to the symmetric stretching vibrations of the  $\text{SiO}_4$  tetrahedra with one nonbridging oxygen (NBO) atom ( $Q^3$  units); 920–950  $\text{cm}^{-1}$  is due to the Si–O $^-$  stretching with two NBO ( $Q^2$  units); 900  $\text{cm}^{-1}$  is attributed to the stretching vibration of  $Q^1$  units with three nonbridging oxygens; and 850  $\text{cm}^{-1}$  is due to the symmetric stretching mode of  $Q^0$  anions (McMillan 1984). Figure 5a shows the infrared bands with vibrational modes. Nuclear magnetic resonance (NMR) study also predicts  $Q^0, Q^1, Q^2, Q^3, Q^4$  notation in silica, and the numbers 0–4 denote the number of ‘Si’ units connected through the oxygen to the other single silicon atom.  $Q^0, Q^1, Q^2, Q^3$  are referred to as a silicon atom with zero, one, two

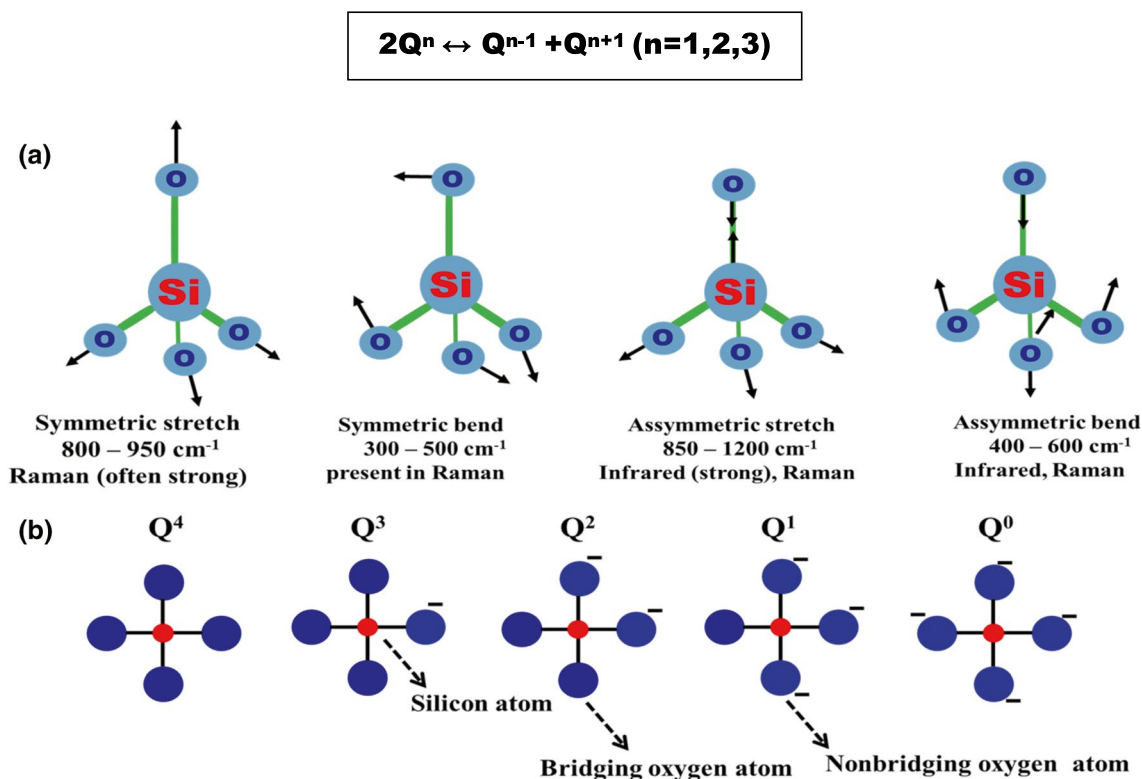
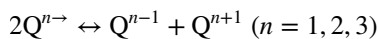


**Fig. 5** a Major vibrational modes for a nonlinear group. b 2D Representation of  $Q^n$  species. Modified after Salh (2011) and Osipov et al. (2015)

and three attachments of another silicon atom, respectively (Lunevich et al. 2016). A schematic two-dimensional representation of the  $Q^n$  species is shown in Fig. 5b.



## Preparation of silica nanoparticles

Various preparation methods are available to synthesize silica nanoparticles, such as microemulsion processing (Finnie et al. 2007), chemical vapor deposition (Rezaei et al. 2014), combustion synthesis (Yermekova et al. 2010), plasma synthesis (Saito et al. 2018), hydrothermal techniques (Gu et al. 2012) and sol–gel processing (Prabha et al. 2019). Major researches efforts have focused on controlling the size and morphology of nanoparticles (Brinker and Scherer 2013). During chemical vapor condensation (CVC), inorganic precursors, e.g., silicon tetrachloride ( $\text{SiCl}_4$ ), are decomposed by a high-temperature flame or react with hydrogen and oxygen to yield silica nanoparticles (Silva 2004; Vansant et al. 1995). The main drawback of flame synthesis is the difficulty in controlling the phase composition, particle size and morphology (Klabunde 2001), yet flame synthesis is the major method for producing silica nanoparticles commercially in powder form. The different methods for silica nanoparticle preparation are presented in Table 1.

## Chemical method

The sol–gel technique has advantages of yielding pure, homogeneous materials, and enabling to obtain various forms of materials such as fibers, films, submicron powders and monoliths (Fardad 2000; Brinker and Scherer 2013). The sol–gel process is defined as the chemical transformation from colloidal suspension of sol into a 3D interconnecting network of gel. In this process, a metal alkoxide undergoes hydrolysis and polymerization reactions to form the sol. Further, the sol allows to preparing the materials in various forms such as discrete particles or polymers. The reaction is controlled by the reactants such as alcohol, water and acid/base; the size of the particles is tuned by pH, precursor concentration and temperature (Burda et al. 2005; Yu et al. 2008; Singh et al. 2011a).

Silica nanoparticles are synthesized by the sol–gel-assisted, low-temperature Stöber method. In this process, the hydrolytic condensation reaction of Si–OH coupling occurs by replacement of an alkoxide group (–OR) with a hydroxyl group (–OH) (Kim et al. 2017). In the beginning, Stöber et al. prepared 1  $\mu\text{m}$  of silica nanoparticles using

the sol–gel method (Stöber et al. 1968). Then, a hundred nanometers to a few micrometers silica nanoparticles were obtained by controlling the concentration of the precursor during hydrolysis (Bogush et al. 1988). The Stöber method also allowed to synthesize various shapes of silica nanoparticles such as nanocubes and spheres. The cubic shape of silica nanoparticles is obtained by addition of tartaric acid during synthesis (Yu et al. 2005), whereas monodisperse nanocubes of silica nanoparticles are prepared using ammonium tartrate as a surface-specific template in the sol–gel method (Yu et al. 2005).

The influence of synthesis parameters on the size and shape of silica nanoparticles has been largely studied. The concentration of the precursor, e.g., tetraethylorthosilicate, and the alcohol, e.g., ethanol, both control the size and distribution of silica nanoparticles. Particle sizes of 1.5 nm and 20–1000 nm were obtained by tuning the concentrations of alcohol and the precursor (Shimura and Ogawa 2007; Wang et al. 2010). Reaction temperature and time, and rotation per minute are also controlling the homogeneous distribution (Dabbaghian et al. 2010). Particle sizes of 50–800 nm and 32–300 nm were obtained by varying the reaction temperature and time (Novak et al. 2010; Kim et al. 2017). Narrow particles can be obtained by controlling the reaction parameters in the Stöber method.

In the wet chemical synthesis, the surfactant allows to tune the size of the particle and prevent agglomeration. Amorphous silica nanoparticles of 300–400 nm were prepared using polyvinyl pyrrolidone, cetyltrimethylammonium bromide (CTAB) and sodium dodecyl sulfate (Stanley and Nesaraj 2014). Particle size of 9 nm was obtained using polyethylene glycol-100 as a surfactant (PEG 1000, Guo et al. 2017). The properties of silica nanoparticles can be tuned also during sol–gel-assisted sonication. Particle size decreases with increased concentration of reagents, e.g.,  $\text{NH}_3$ , tetraethylorthosilicate, ethanol and water, by ultrasonication during the sol–gel process (Rao et al. 2005). Further functionalization of silica nanoparticles allows applications in nanomedicine and the industry (Lieberman et al. 2014; Dubey et al. 2015).

The main parameters controlling the size and shape of silica nanoparticles are concentrations of tetraethylorthosilicate (TEOS), ammonia hydroxide ( $\text{NH}_4\text{OH}$ )/ammonia ( $\text{NH}_3$ ), water, ethanol and reaction temperature (Bogush et al. 1988; Rao et al. 2005). Table 2 presents factors controlling particle size. Overall, particle size increases with tetraethylorthosilicate concentration (Sumathi and Thenmozhi 2016), ethanol concentration (Singh et al. 2014a), pH of the reaction (Singh et al. 2011a) and reaction temperature (Zainala et al. 2013). Particle size also increases with increasing concentration of  $\text{H}_2\text{O}$ , yet as  $\text{H}_2\text{O}$  concentration increases the size of some particles decreases. This is because  $\text{H}_2\text{O}$  accelerates tetraethylorthosilicate

**Table 1** Methods for preparation of silica nanoparticles

Methods	Synthesis	Observation
Chemical method	Sol–gel	Hydrolysis and condensation of metalalkoxides and inorganic salts such as tetraethylorthosilicate and sodium silicate with acid or base as catalyst Prepared spherical shape of 7–200 nm Sizes tuned by temperature, reagent concentration and pH Lower time of reaction
	Wet chemical	Same reagents as sol gel method plus surfactants such as polyvinyl pyrrolidone, cetyltrimethylammonium bromide, sodium dodecyl sulfate Amorphous product Surfactant used to tune size Longer reaction time
	Precipitation	Silica gel made using sodium hydroxide and sulfuric acid Spherical particles 50 nm size Long reaction time
Biomass	Corn cob Rice husk Sugarcane bagasse	Initial extraction by acid and thermal treatments Nanosilica prepared from biomass by precipitation or sol gel processes
Mesoporous silica	Soft templating method	Mesoporous silica increases loading capacity in drug delivery
	Single micelle-templating	Organosilica and ethylene-bridged organosilica precursors Pluronic triblock, pluronic F127 block and cationic block copolymer as templates
	Vesicle-templating	Mixture of silicates and silanes as anionic co-surfactants and cationic surfactants Requires uniform particles size of 25–105 nm obtained by co-condensation Tetraethylorthosilicate (TEOS) and organotriethoxysilanes in alkaline solution. Cationic surfactant: cetyltrimethylammonium chloride
	Micro-emulsion-templating	Emulsion obtained by mixing oil, water, surfactant and alkaline solution Thermally stable particles obtained using water, cationic surfactants and hydrocarbons
	Hard templating method	Mono-dispersed mesoporous silica nanoparticles obtained using polymer lattices, metal oxides and silica colloids
	Polymer latex-templating	Selective functional groups activated by surface activation for silicification Functional groups activation achieved by layer-by-layer deposition through electrostatic attraction
	Metal or metal oxide nanoparticles	Cetyltrimethylammonium bromide (CTAB) acts both as stabilizer and mesostructural directing agent Thickness of mesoporous silica shells tuned by varying the ratio of surfactant and silica precursor
Core–shell silica		Core is coated with non-toxic material to make nanoparticles biocompatible Shell layer reduces toxicity and enhances the properties of the core material

hydrolysis; and H<sub>2</sub>O dilute oligomers in the reaction, which helps to produce larger particles and smaller particle, respectively (Wang et al. 2010). Finally, a narrow distribution of particle size is obtained at high concentrations of ammonia (Zeng et al. 2015). While the mechanism corresponding to the nucleation and growth of silica nanoparticles still needs to be explained, a well understanding of

the impact of synthesis parameters on the resultant particle size and shape is gradually developing.

Table 3 shows chemical methods of silica nanoparticle preparation. The influence of the chemical reagents on particle size, distribution and morphology is given as scanning electron microscopy and transmission electron microscopy images in Figs. 6 and 7, respectively.

**Table 2** Parameters controlling particle size of silica nanoparticles (Rao et al. 2005)

Parameter	Experimental condition					Size (nm)
	Ethanol (mol L <sup>-1</sup> )	Tetraethylortho-silicate (mol L <sup>-1</sup> )	H <sub>2</sub> O/tetraethyl-orthosilicate (mol L <sup>-1</sup> )	NH <sub>4</sub> OH (mol L <sup>-1</sup> )	Temp. (°C)	
Effect of ethanol	4–8	0.045	66.7	14	–	20.5 < <i>d</i> < 224.2
Effect of tetraethyl orthosilicate (TEOS)	8	0.012–0.11	27–311	14	–	60.1 < <i>d</i> < 417
Effect of ammonia (NH <sub>4</sub> OH)	8	0.045	66.7	2.8–28	–	242.8 < <i>d</i> < 30.6
Effect of water	8	0.045	66.7 209	14	–	224.2 < <i>d</i> < 20.5
Effect of temperature	4–8	0.045	66.7	14	30 70	116.0 < <i>d</i> < 462.03

*Temp.* Temperature, *d* diameter

**Table 3** Synthesis of silica nanoparticles by chemical methods

Method	Observation	References
Stober: fixed ammonia (NH <sub>3</sub> )/H <sub>2</sub> O/ ethanol mole amounts, varied mass of tetraethyl orthosilicate (TEOS)	Silica opals with diameters 480 nm and 540 nm;	Razo et al. (2008)
Stober: TEOS: 0.2 M, NH <sub>3</sub> : 0.2 M, H <sub>2</sub> O: 1 M; NH <sub>3</sub> : 0.11 M, TEOS: 0.28 M, H <sub>2</sub> O: 1 M; NH <sub>3</sub> : 0.3 M, TEOS: 0.28 M, H <sub>2</sub> O: 1 M	Particle size 50 nm, 55 nm, 130 nm, respectively. The size of particles increased with increased tetraethyl orthosilicate (TEOS) and ammonia (NH <sub>3</sub> ) concentrations.	Ibrahim et al. (2010)
Sonochemical sol–gel process. Polyethylene glycol 1000 (PEG 1000) surfactant, tetraethyl orthosilicate (TEOS) silicon sources & ammonia (NH <sub>3</sub> ) as a catalyst	Disperse without any agglomeration. Equiaxed in shape. Dispersity, size morphology tuned by varying PEG 1000. Narrow size distribution of 4–18 nm. Average size of 9 nm	Guo et al. (2017)
Stober method—silica nanoparticles with a high concentration. Tetraethyl orthosilicate (TEOS) as a starting material.	10 nm of 4% of silica nanoparticle through reaction condition. By removing solvent, particle concentration increased up to 15 wt.% without aggregation	Tadanaga et al. (2013)
TEOS, ammonia (NH <sub>3</sub> ), H <sub>2</sub> O controls the reaction rate and particle size. NH <sub>3</sub> and H <sub>2</sub> O concentrations control the hydrolysis and the condensation processes.	Monodisperse spherical silica nanoparticles at 20 nm	Beganskienė et al. (2004)
Stober method	A series of nanoparticles with controllable size from 20 to 100 nm	
Silica nanoparticles influence as a function of the temperature, precursor, water and catalyst	Particle size is independent of the concentration of the precursor and depends on the concentration of the ammonia solution. But it is inversely proportional to the reaction temperature	Qi et al. (2017)
Sol–gel method. Varied parameters, aging time 2 to 6 h. Calcination temperature in the range of 600 °C–700 °C	Average size in the range of 79.68 nm to 87.35 nm. Optimum conditions at calcination temperature of 700 °C and 2 h aging time	Azlina et al. (2016)
Micelles entrapment approach. Varying synthesis parameters	The average size of silica nanoparticles depends on the reactants and reaction temperature. The particle sizes of 28.91 nm–113.22 nm through varying the temperature of the reaction. 2-butanol as a solvent	Hajarul et al. (2011)

## Biomass

To prepare silica nanoparticles, most investigations use organic precursors of alkoxysilane such as tetraethyl orthosilicate (TEOS) and tetramethyl orthosilicate (Bosio et al.

2013). Nonetheless, silica from natural resources is used in biomedical and materials fields due to low cost, eco-friendliness and availability. Silica can be successfully extracted from biomass such as sugarcane bagasse, rice husk, corn cob, coffee husk and wheat husk. Rice husk is an abundant

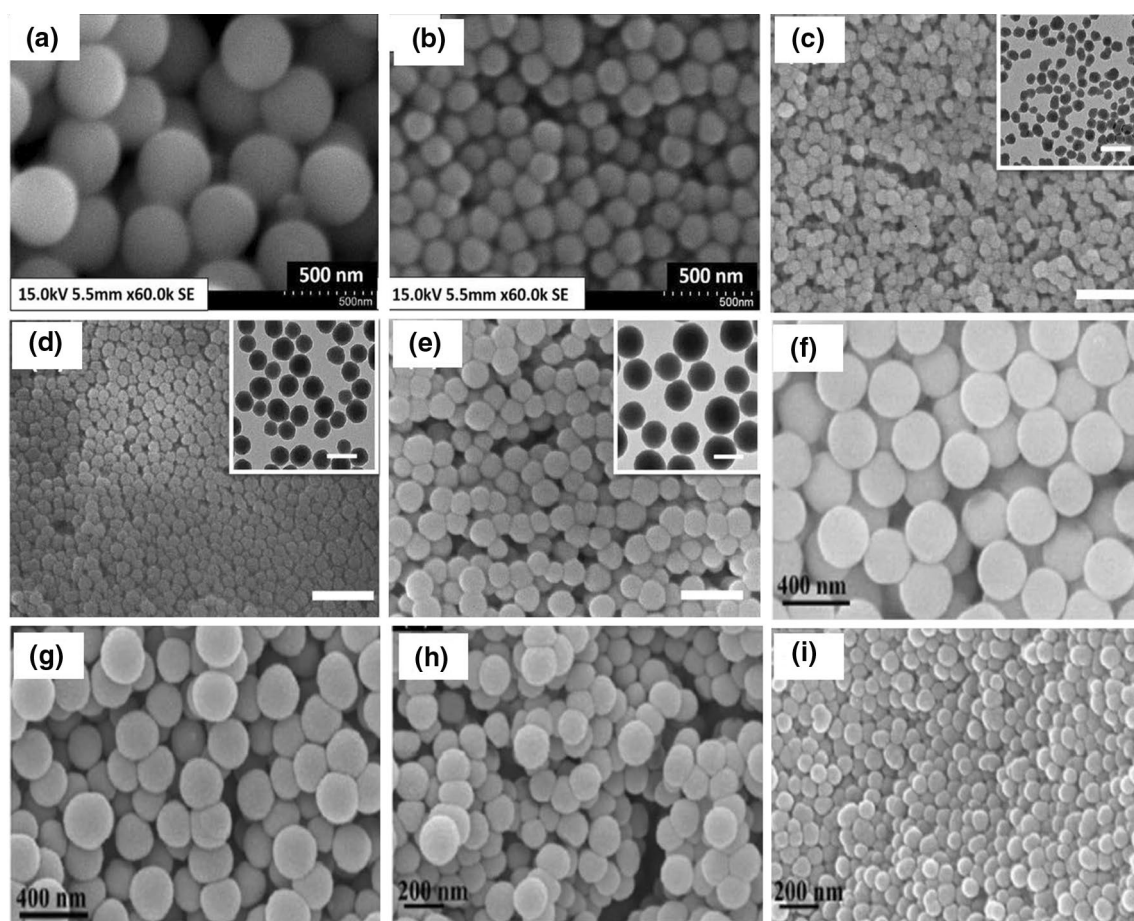


**Fig. 6** Scanning electron microscopy (SEM) of silica nanoparticles with fixed concentration of tetraethylorthosilicate (TEOS) and varied ethanol to water ratios: **a** 4:1, **b** 3:1 (Prabha et al. 2019). Fixed concentration of TEOS, ethanol and water and varied  $\text{NH}_3$  concentrations: **c** 150 mM, **d** 200 mM, **e** 250 mM, reprinted with permission from Zhang et al. (2016). Fixed concentration of  $\text{NH}_3$  and ethanol

and varied  $\text{H}_2\text{O}$  to TEOS ratio: **f** 8:4, **g** 10:4, **h** 12:4, **i** 14:4, reprinted with permission from Kim et al. (2017). Average particle sizes of **a** 450 nm, **b** 200 nm, **c** 30 nm, **d** 50 nm, **e** 90 nm, **f** 280–300 nm, **g** 200–230 nm, **h** 150–180 nm, **i** 100–120 nm. These images reveal that particle size increases with concentration of precursor, solvent and water

silicon source, and contains about 75–90% of cellulose, hemicellulose and lignin totaling and 17–20% of ash content (Azmi et al. 2016). The ash contains more than 90% of silica and few metallic impurities. Sugarcane bagasse ash, a major by-product of the sugarcane industry, contains 40–50% of silica; acid pretreatment allows to increase amount of silica up to 80% (Ganesan et al. 2007; Singh and All Jawald 2013).

Corn cobs, obtained from maize corn, contain more than 60% of silica (Owoeye et al.). Wheat husk ash contains up to 90% silica (Naqvi et al. 2011), which is close to that of dry silica sand, of 99.4%. Bamboo leaf ash also has a large silica content of 75.90–82.86 wt.% (Silviana and Bayu 2018). Raw teff straw contains about 52% of silica, which can be increased to 97% after thermal treatment (Wassie and Srivastava 2017).

Examples of silica-rich biomass are shown in Fig. 8. Extraction of silica from biomass, preparation and characterization of silica nanoparticles are discussed below.

### Corn cob

Corn is one of the most frequently grown food crops in the world; it is extracted from maize (corn). Corn cob ash contains more than 60% of silica and few metallic elements (Adesanya and Raheem 2009). Corn cob is grounded to a fine powder that is used to produce silica, silicates and silica nanoparticles. Corn cob is used for enzymes, absorbents (Tsai et al. 2001), proteins (Chen et al. 2007), fuel



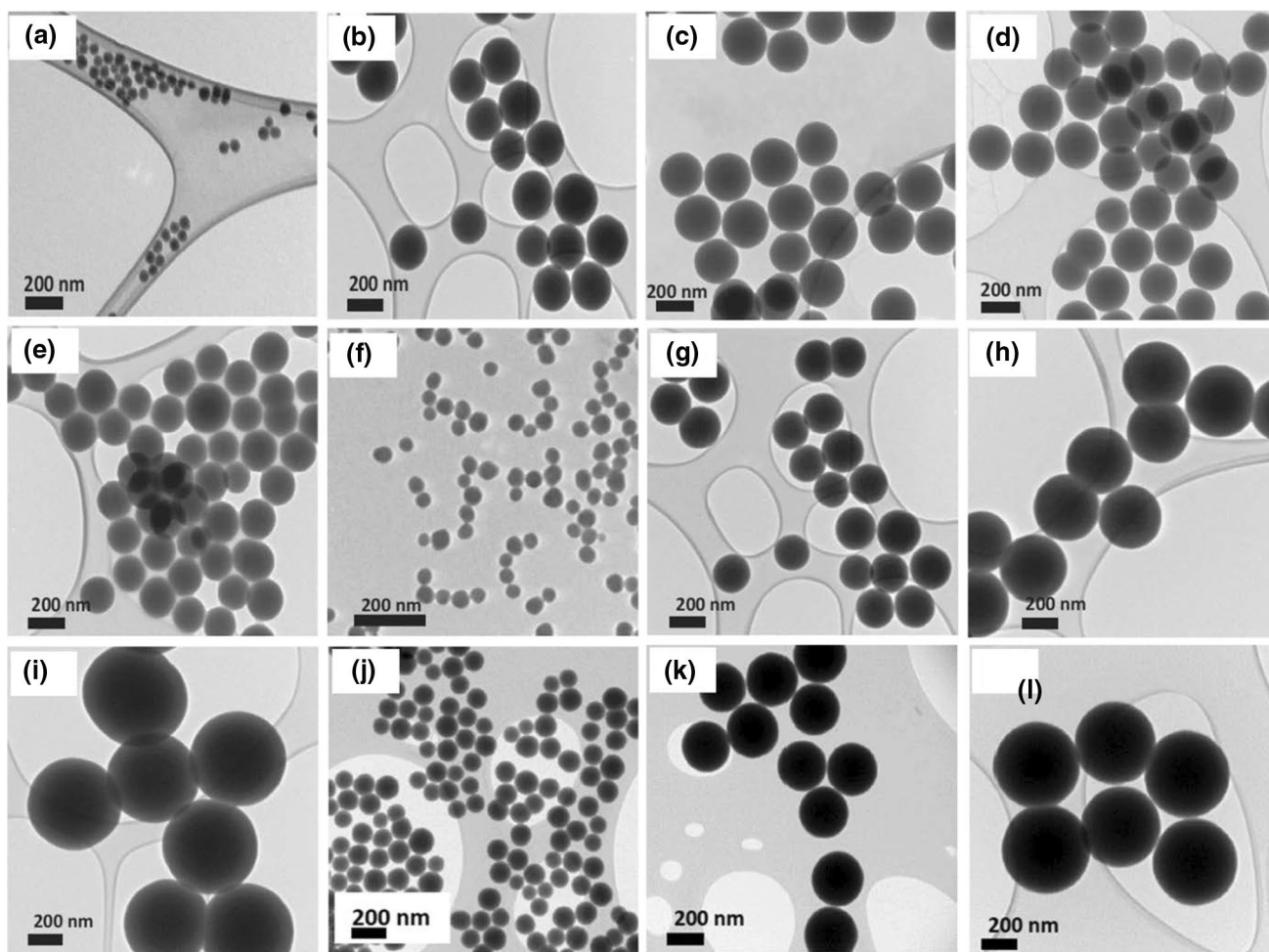


**Fig. 7** Transmission electron microscopy (TEM) of silica particles. **a–d** fixed concentration of tetraethylorthosilicate (TEOS), ammonia solution (NH<sub>4</sub>OH) and varied amounts of water. Fixed concentration of TEOS and water, and varied concentration of NH<sub>4</sub>OH **f** 0.11 M, **g** 0.28 M, **h** 0.57 M, **i** 1.13 M, **j** 0.17 M, **k** 0.40 M, **l** 0.85 M, reprinted

with permission from Greasley et al. (2016). NH<sub>4</sub>OH concentration controls the density of the silica particles. The narrow distribution of particle size obtained at higher ammonia concentration and H<sub>2</sub>O could accelerate TEOS hydrolysis and helps to produce larger particles



**Fig. 8** Biomass sources having high content in silica

(Kaliyan and Morey 2010) and cement (Adesanya and Raheem 2009). The chemical composition of raw corn cob ash and extracted silica is shown in Table 4 (Okoronkwo et al. 2013).

Nanosilica is prepared from corn cob ash by precipitation (Mohanraj et al. 2012). The 50–60% of silica in corn cob ash must be purified to remove of impurities. Silica aquagel from corn cob ash is prepared by alkaline extraction and acid

**Table 4** Chemical composition of raw corn cob ash and extracted silica. Source: Okoronkwo et al. (2013)

Constituent	Raw corn cob ash (wt. %)	Extracted silica (wt. %)
Silicon dioxide (SiO <sub>2</sub> )	47.66	97.13
Aluminum oxide (Al <sub>2</sub> O <sub>3</sub> )	8.50	0.00
Iron oxide (Fe <sub>2</sub> O <sub>3</sub> )	7.90	0.48
Calcium oxide (CaO)	17.70	0.89
Magnesium oxide (MgO)	7.20	0.92
Sulfur trioxide (SO <sub>3</sub> )	0.70	0.00
Manganese oxide (MnO <sub>2</sub> )	2.20	0.00
Potassium oxide (K <sub>2</sub> O)	4.80	0.58

precipitation (Velmurugan et al. 2015). Silica can be isolated from corn cob by varying pH (7–10) using the sol–gel method (Shim et al. 2015). The results show a 99.50% purity, larger surface area, high reactivity and 98.50% amorphous state. Scanning electron microscopic (SEM) images of corn cob and silica nanoparticles are displayed in Fig. 9.

Silica nanoparticles from corn cob extracts are also prepared by precipitation. Here, soluble sodium silicate solution from corn cob ash is used as a source of silica, and concentrated sodium hydroxide (NaOH) is used as a source of soda. Various parameters such as specific gravity, pH value, viscosity and electrical conductivity were studied (Ajayi and

Owoeye 2015). Silica nanoparticles prepared from corn cob yield amorphous silica with large surface area.

## Rice husk

Rice husk has been studied for energy and for production of silica (Liu et al. 2016a, b). For instance, rice husk ash is a precursor for silica gel synthesis by the sol–gel method: here sodium silicate is prepared first then converted into a gel by acid treatment (Geetha et al. 2016). Acid and thermal treatments yield a white color silica with high surface area (Della et al. 2002). Rice husk has about 20% of minerals (Carmona et al. 2013). Organic compounds include cellulose, hemicellulose and lignin. Minerals contains 94% of silica and 6% of Al<sub>2</sub>O<sub>3</sub>, K<sub>2</sub>O, MgO, CaO and P<sub>2</sub>O<sub>5</sub>. Composition varies depending on soil type, fertilizers and weather conditions (De Souza et al. 2002). The chemical composition of rice husk is shown in Table 5.

For optimal production of nanosilica from rice husk, the effect of the acid leaching, concentration of sodium silicate solution, reaction temperature and time of aging and gelation, pH on synthesizing silica nanoparticle, were studied (Liou and Yang 2011). Research also focused on morphology of rich husk ash, which displays a porous structure after washing, acid treatment and sintering (Madrid et al. 2012). As a consequence, rich husk ash shows promising

**Fig. 9** Scanning electron microscopy of **a** corn cob, reprinted with permission from Shariff et al. (2016), **b** calcined corn cob ash obtained at 650 °C for 2 h, **c** nanosilica from corn cob, reprinted with permission from Mohanraj et al. (2012), **d** nano-structured silica from corn cob with an average diameter of 55 nm, reprinted with permission from Okoronkwo et al. (2016)

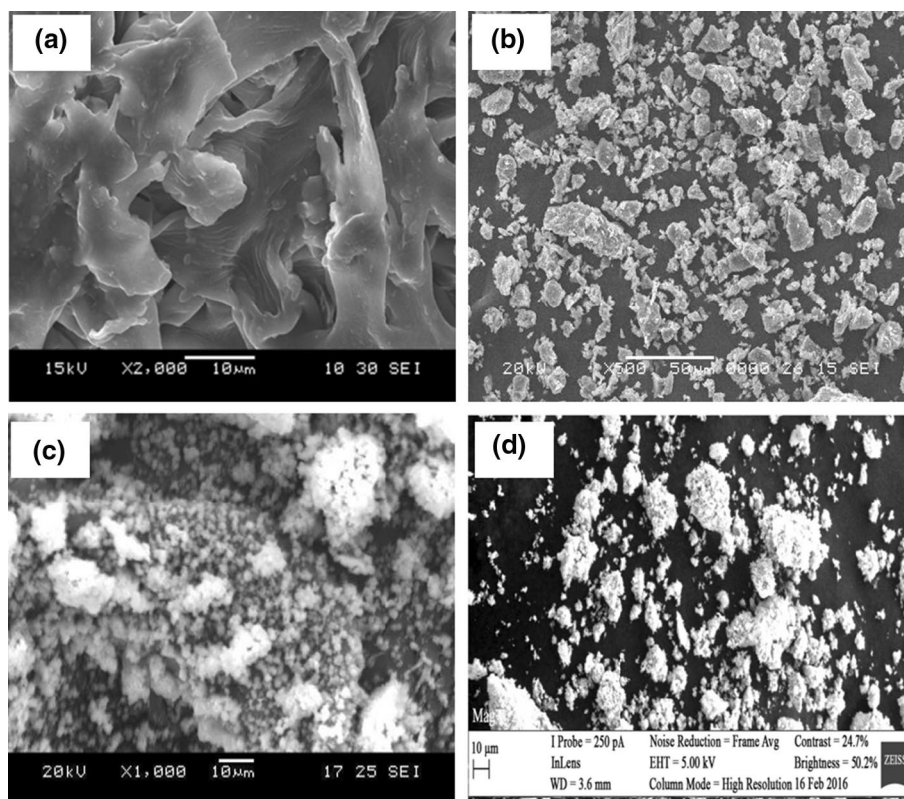


**Table 5** Composition of rice husk ash (Ramadhansyah et al. 2012)

Oxide compounds	Chemical composition (%)
Silicon dioxide (SiO <sub>2</sub> )	93.0
Aluminum oxide (Al <sub>2</sub> O <sub>3</sub> )	0.20
Iron oxide (Fe <sub>2</sub> O <sub>3</sub> )	0.13
Calcium oxide (CaO)	0.49
Magnesium oxide (MgO)	0.73
Sodium oxide (Na <sub>2</sub> O)	0.02
Potassium oxide (K <sub>2</sub> O)	1.30
Sulfur trioxide (SO <sub>3</sub> )	0.15
Loss on ignition (LOI)	3.98

applications for construction materials and technical ceramics due to the high reactivity of the porous structure.

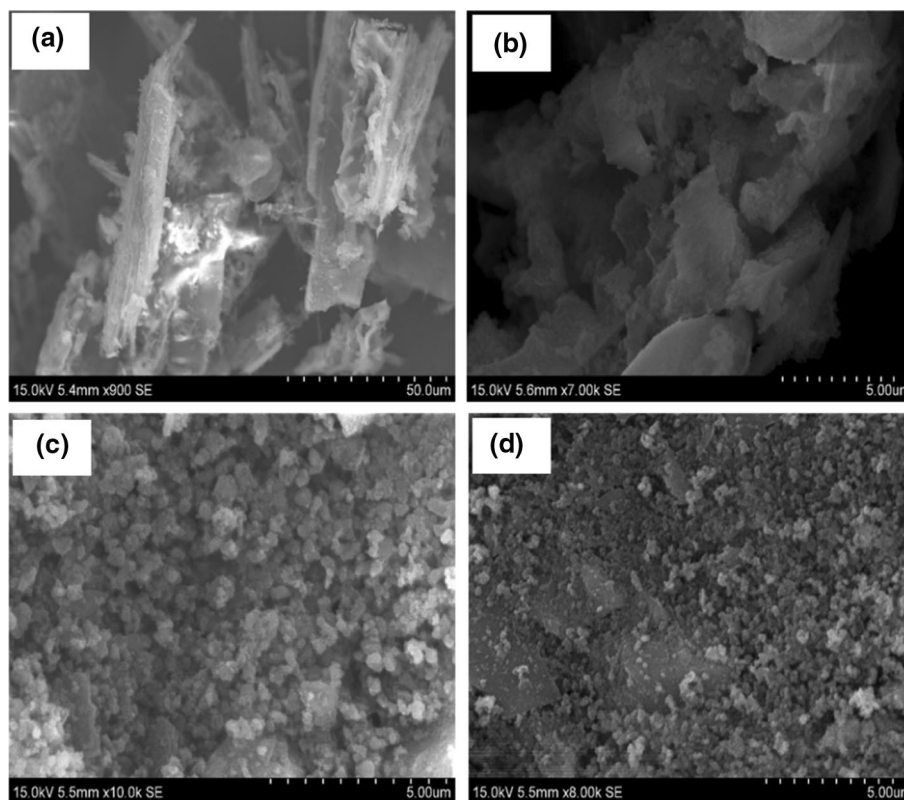
Extraction and characterization of silica from a different rice husks such as agulhinha and cateto were analyzed (Carmona et al. 2013). Highly pure silica nanoparticles with high specific area and an average size of 25 nm were prepared by alkali extraction, followed by acid precipitation (Yuvakkumar et al. 2014). Research has also focused on ‘waste in valuable product manufacture’ using silica, revealing good performance and simple industrial implementation as anti-sticking agents, filter in rubber products

and paper (Todkar et al. 2016). Silica nanocomposite can be prepared with rice husk ash, which is used as a nano-filler in epoxy-silica nanocomposites; products display good tensile strength, uniform distribution and no agglomeration (Moosa and Saddam 2017). To synthesize high surface area silica aerogel from rice husk ash, the water extract of rice husk is used as a precursor in the sol-gel process (Feng et al. 2018). The image of rice husk, after acid leach of rice husk, and the morphology of rice husk ash and silica nanoparticles are shown in Fig. 10. Overall, rice husk silica can be used to develop valuable products, thus solving the disposal issue (Tyagi et al. 2017).

## Sugarcane bagasse

India has the second largest manufacture of sugarcane in the world. Bagasse is the residue of sugarcane; bagasse is obtained industrially by milling. India produces 10 million tons of sugarcane bagasse ash as a waste material (Goyal et al. 2007). Silica is abundant in sugarcane bagasse ash (Aigbodion et al. 2010; Faria et al. 2012). Mesoporous silica nanoparticles prepared from sugarcane bagasse are applied in biomedical and industrial fields (Rahman et al. 2015). Sugarcane bagasse is considered as a better option

**Fig. 10** Scanning electron microscopy. **a** rice husk. Silica nanoparticles synthesized from rice husk under various conditions giving: **b** particles in heterogeneous sizes, **c** agglomeration, **d** 50 nm size (Prabha et al. 2019)



than wood fibers in producing textiles, paper, pressed wood materials and other products (Mandal and Chakrabarty 2011). Silica extracted from sugarcane is suitable as additive for membrane fabrication (Mokhtar et al. 2016). In the nineteenth century, silica was found in plants, and then, silica is generally accepted as a sustainable polymer compound (Hariharan and Sivakumar 2013). The chemical composition of sugarcane bagasse ash is shown in Table 6 (Chusilp et al. 2009).

The effect of calcination temperature and alkali concentration on silica structure have been studied (Rahmat et al. 2016; Athinarayanan et al. 2017). HCl is used for washing, and NaOH was for silica extraction. Acid pretreatment in autoclave removes metal ions and induces the hydrolysis

of organic substances. Bagasse ash filler treated with HCl/ $\text{NH}_4\text{F}$  gives silica of 77%–97% purity (Huabcharoen et al. 2017). SEM images of the sugarcane bagasse, bagasse ash and silica nanoparticles from sugarcane bagasse are shown in Fig. 11.

## Mesoporous silica

Porosity is classified according to pore size (Table 7, Barabino 2011). Porosity is defined as the periodic arrangements with uniform size mesopores integrated within the amorphous silica matrix.

Mesoporous silica material was discovered in 1992 by the Mobil Oil corporation and is known as the M41S phase having pore diameters from about 2 to 10 nm (Hoffmann et al. 2006). The materials are often referred to as Mobil composition of matter (MCM) (Caras 2011), and the most popular MCM materials are MCM-41 and MCM-48,

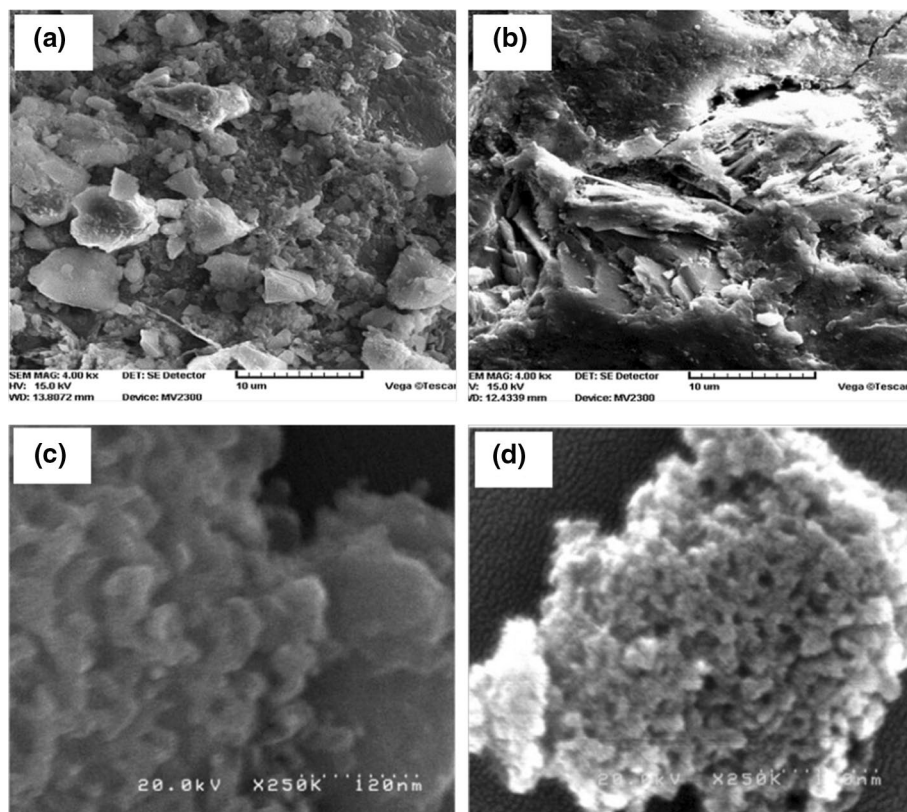
**Table 6** Chemical composition of sugarcane bagasse ash (Chusilp et al. 2009)

Chemical composition (%)	Sugarcane bagasse ash
Silicon dioxide ( $\text{SiO}_2$ )	64.88
Aluminum oxide ( $\text{Al}_2\text{O}_3$ )	6.40
Iron oxide ( $\text{Fe}_2\text{O}_3$ )	2.63
Calcium oxide (CaO)	10.69
Magnesium oxide ( $\text{MgO}$ )	1.55
$\text{SiO}_2 + \text{Al}_2\text{O}_3 + \text{Fe}_2\text{O}_3$	73.91

**Table 7** Classification of porous material (Hoffmann et al. 2006)

Types of porous material	The diameter of pores (nm)
Microporous	Diameter < 2
Mesoporous	2 < diameter < 50
Macroporous	Diameter > 50

**Fig. 11** Scanning electron microscopy of 15% sugarcane bagasse at ages of **a** 7 days and **b** 28 days, with scale bar of 10  $\mu\text{m}$ . Reprinted with permission from Joshaghani et al. (2017). **c** Silica-polyethylene glycol (PEG) hybrid. **d** porous silica after PEG extraction. Reprinted with permission from Rahman et al. (2015)



displaying 2D hexagonal and 3D cubic arrangement of pores, respectively (Tzankov et al. 2014). Mesoporous silica got high interest due to tunable particle size (10–1000 nm) and pore diameter (2–30 nm), large surface area and pore volume, flexible morphology, surface functionalization and uniform mesoporosity, tunable and narrow pore size distribution, and excellent biocompatibility and biodegradation. Mesoporous silica nanoparticles (MSNPs) have been developed for inorganic delivery (Caras 2011). Mesoporous silica nanoparticles have sizes ranging from 50 to 500 nm in diameter with pores ranging from 2 to 20 nm; these pores are mainly cylindrical (Kresge et al. 1992). Pores act as vehicles and reservoirs in a wide range of fields such as drug delivery, adsorption and heterogeneous catalysis. Applications include drug delivery of therapeutic agents (Thomas et al. 2010; Slowing et al. 2007; Trewyn et al. 2007).

Microscopic images of mesoporous silica obtained by various methods are shown in Fig. 12. Mesoporous silica nanoparticles are prepared using amphiphilic molecules as templates for their internal structure. Two different structures can be obtained by changing the synthesis conditions, the two-dimensional hexagonal structure known as MCM-41 (Beck et al. 1992; Kresge et al. 1992) and the tridimensional cubic structure MCM-48 (Hoffmann et al. 2006). Mesoporous silica materials were first synthesized

for catalytic applications (Yanagisawa et al. 1990; Kresge et al. 1992). To increase biocompatibility, smaller sizes and homogeneous morphology are required. For instance, submicrometer MCM-41 particles were prepared in 1997 by a modified Stober method (Grün et al. 1997). Later, 100 nm MCM-41 silica particles were synthesized using a dilute surfactant solution (Cai et al. 2001), and then, less than 50 nm particles were prepared by dialysis (Suzuki et al. 2004). Overall, mesoporous silica nanoparticles have large pore volume and surface area and can be functionalized with versatile functional groups for theranostic applications.

### Core-shell silica

Core-shell nanoparticles refer as inner material coated with another material on the surface (Law et al. 2008). Core-shell nanoparticles have numerous advantages over conventional nanoparticles in biological applications because these particles display high dispersibility and low cytotoxicity, bio- and cytocompatibility, better conjugation with other bioactive molecules, and increased thermal and chemical stability (Sounderya and Zhang 2008). The core is coated with non-toxic material to make nanoparticles biocompatible. The shell layer reduces the toxic layer and

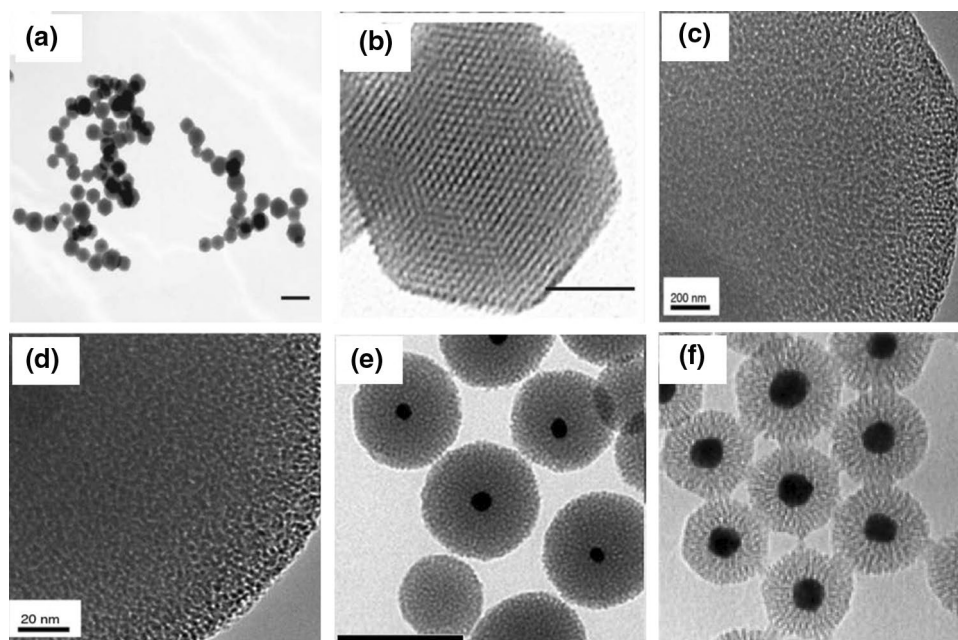


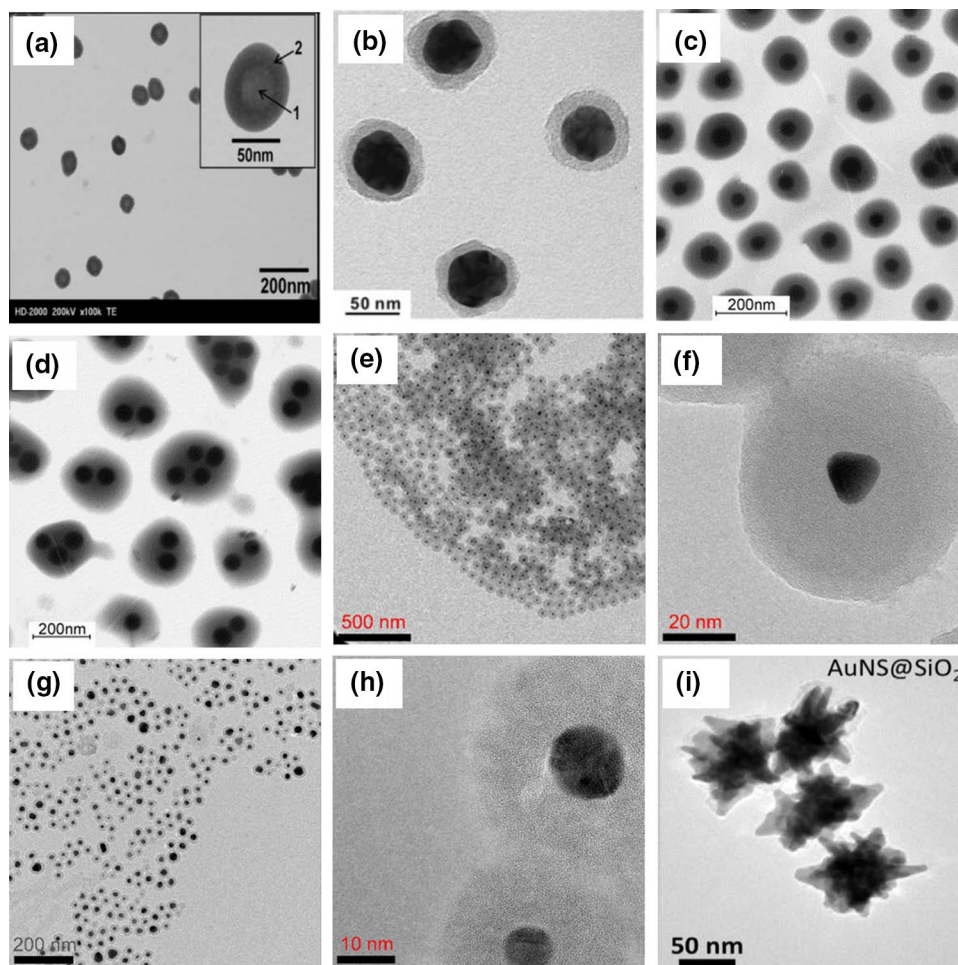
**Fig. 12** Transmission electron microscopy (TEM) of **a** mesoporous silica nanoparticle with an average diameter of 120 nm. **b** High-resolution image of a single particle, pore size 2.7 nm, reprinted with permission from Yu et al. (2011). **c** 0.1 M CTAB:45 M H<sub>2</sub>O pore size 2.9 nm. **d** 0.1 M CTAB:45 M H<sub>2</sub>O pore size 2.7 nm, reprinted with permission from Vazquez et al. (2017). **e** Gold-mesoporous silica

under plasmonic photothermal with irradiation for 14 h at 514 nm under 15 mW, reprinted with permission from Croissant and Guardado-Alvarez (2019). **f** Multibranching-polymer composite with gold-silica core-shell nanoparticles, reprinted with permission from Carasco et al. (2016). CTAB: cetyltrimethylammonium bromide

enhances the properties of the core material (Chatterjee et al. 2014). Core–shell nanoparticles are mainly designed to increase the binding affinity with ligands, drugs and receptors in biomedical applications (Sahoo and Labhassetwar 2003; Gilmore et al. 2008; Chen et al. 2010). The thickness of the shell can be tuned to improve contrast agents, targeted drug delivery, specific binding and biosensing (Pinho et al. 2010). Microscopic images of silica

nanoparticles with a core–shell structure are shown in Fig. 13. Tables 8 and 9 present core–shell silica nanoparticles for biosensor and bioimaging applications.

**Fig. 13** Transmission electron microscopy. **a** Silica–gadolinium particle, reprinted with permission from Kobayashi et al. (2007). **b** Silver–silica with silica shell thickness of  $8 \pm 2$  nm (Song et al. 2016). Core–shell of polystyrene–silica composites (PSC), **c** silica: styrene 1:10, **d** silica:styrene 1.5:10, reprinted with permission from Ding et al. (2004). Core–shell of gold–silica at various scales: **e** 500 nm, **f** 20 nm. Gold–silica with template of 0.1 g cetyltrimethylammonium bromide (CTAB) at various scales: **g** 200 nm, **h** 10 nm, reprinted with permission from Vu et al. (2019). **i** Core–shell of Au nanostar–silica nanoparticles, reprinted with permission from Al-Ogaidi et al. (2014)

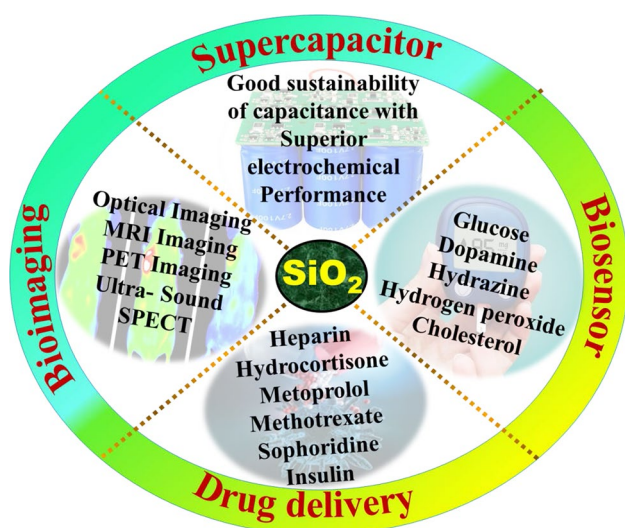


**Table 8** Core–shell silica nanoparticles for biosensor applications

Core	Shell	Application	References
Gold nanostar	Silica nanoparticle	Glucose sensor	Al-Ogaidi et al. (2014)
Teardrop-shaped silica nanoparticles	Titanium dioxide nanoparticles	For photocatalytic activity	Wu et al. (2015)
Silver nanoparticles	Silica nanoparticles	Aptasensor	Song et al. (2016)
DNA-labeled silicon	Silica nanoparticles	Fluorescent sensor for detection of $Hg^{2+}$ in water	Srinivasan et al. (2017)
$Fe_3O_4$ nanoparticles	Inner shell: amorphous carbon. Outer shell: metallic silver nanoparticles	Cholesterol nanobiosensors	Satvekar and Pawar (2018)
Gold nanoparticles	Silica nanoparticles and 4,4'-dipyridyl embedded into the core–shell	Detection of <i>E. coli</i> O157: H7	Zhu et al. (2018)

**Table 9** Core–shell silica nanoparticles for bioimaging application

Core	Shell	Application	References
Gadolinium	Silica nanoparticle	X-ray imaging	Morimoto et al. (2011)
Iron oxide	Silica with different thicknesses	Multimodal molecular imaging: MRI and optical imaging	Jang et al. (2014)
Gadolinium	Mesoporous silica	Drug delivery	Stefanakis and Ghanotakis (2014)
Quantum dot	Silica nanoparticle	Contrast agent with dual functions fluorescence and X-ray absorption	Kobayashi et al. (2016)
Monodisperse silica nanoparticle	amorphous gadolinium and europium oxides with mesoporous silica	Drug delivery, fluorescence and magnetic resonance imaging	Eurov et al. (2015)

**Fig. 14** Applications of silica nanoparticles

## Applications of silica nanoparticles

Silica nanoparticles are used in many fields such as biomedical, electrical, textile and rubber sectors, yet nowadays research is moving toward the biomedical field. Here silica nanoparticles are used in diagnosis and to control diseases by identifying and correcting the genetic disorders, as a theranostics agent. In addition, some applications such as biosensor, bioimaging, drug delivery and supercapacitor are briefly discussed. Applications of silica nanoparticles are shown in Fig. 14 and Table 10.

## Biosensors

Sensors are the analytical device that consists of an active sensing material with a signal transducer (Kuswandi 2019). In general, sensors can be categorized into two types: biosensors and chemical sensors. This classification is based on

sensing aspects, where the biosensors can sense biochemical compounds such as enzymes (Verma 2017), antibodies, nucleic acids, cells and tissues (Yogeswaran and Chen 2008). Biosensors typically consist of two intimately associated elements: a bioreceptor and a transducer. Based on the transducing mechanism, biosensors are further classified as (i) optical-detection biosensors, (ii) resonant biosensors, (iii) thermal detection biosensors, (iv) ion-sensitive field-effect transistor-based biosensors and (v) electrochemical biosensors (Chaubey and Malhotra 2002). Numerous electrochemical biosensors have been developed for determining various substances such as glucose (Saei et al. 2013), cholesterol (Hui et al. 2015), dopamine (Huang et al. 2015), hydrazine (Liu et al. 2016a, b), hydrogen peroxide (Ju and Chen 2015), kanamycin (Qin et al. 2016) and cysteine (Amiri et al. 2017). Optical biosensors are applicable in environmental monitoring, biomedical research, pharmaceuticals, healthcare, homeland security and the battlefield due to powerful detection and analysis tools (Amiri et al. 2017).

For non-enzymatic detection of hydrogen peroxide ( $H_2O_2$ ), graphene oxide was composited with silica nanoparticles (Huang and Li 2013). Amperometric studies show that composites of graphene oxide and silica nanoparticles enhance the electrochemical activity of hydrogen peroxide detection in alkaline medium, with a low detection limit of 2.6  $\mu M$  and high reproducibility. Functionalized mesoporous silica is used for detection of  $H_2O_2$  and controlled treatment of heart failure (Tan et al. 2017). Here, the  $H_2O_2$ -sensitive probe is attached to the surface of a mesoporous silica nanoparticles (MSNP), and captopril, a drug for heart failure, is loaded inside the pores of nanoparticles. A MSNP-based system of high loading efficiency and releasing capacity was developed and combined with detection by chemiluminescence of luminol / hydrogen peroxide (Chen et al. 2016). For dengue RNA detection, 3-aminopropyltriethoxysilane (APTES)-functionalized graphene oxide was enclosed in silica nanoparticles (Jin et al.

**Table 10** Applications of silica nanoparticles

Material	Application	Process
Gold nanoparticles-mesoporous silica composite	Glucose Biosensor	Combining gold nanoparticles-mesoporous silica. Biosensor made by immobilizing $\text{IO}_4^-$ -oxidized-glucose oxidase on gold nanoparticles-mesoporous silica. Modified gold electrode with 2-aminoethanethiol as a cross-linker (Bai et al. 2007)
Hollow silica spheres	DNA Biosensor	Depositing gold nanoparticle/hollow silica spheres on a screen-printed carbon paste electrode for the detection of <i>E.coli</i> DNA. Using glutaraldehyde bifunctional cross-linker, an aminated DNA probe is coupled to the aminated hollow silica spheres and deposited onto the electrode of gold nanoparticle-modified screen-printed carbon paste (Ariffin et al. 2018)
TAT (cell penetrating peptide) conjugated with fluorescein isothiocyanate and doped silica nanoparticles	Bioimaging	Human lung adenocarcinoma (A549) cells (in vitro) and rat brain tissue (in vivo) tagged with nanoparticles. Endovascular approach targets brain blood vessels to study blood–brain barrier (Santra et al. 2004)
Carbon dots inserted in a silica shell around polylactide-polyethylene-glycol conjugated silica core	Bioimaging	Fluorescence induced by incorporation of carbon dots into silica nanoparticle shell. Carbon dots with silane groups on the silica shell using a one-pot reaction. For cellular uptake, silica-loaded core are incubated with A549 cells line and studied for drug release and bioimaging. Silica core–shell material proved promising materials for both bioimaging and anticancer drug delivery (Mehdi et al. 2018)
Mesoporous MCM-41 silica	Drug delivery	Mesoporous MCM-41 is loaded with ibuprofen. Drug release in a simulated body fluid. Drug release analyzed in amine-functionalized MCM-41 of micro-sized sphere and irregular shape. Non-functionalized mesoporous silica shows lower drug release. For amine-functionalized mesoporous silica, drug release rate is better for spherical shape compared to irregular shape (Manzano et al. 2008)
Mesoporous silica nanoparticles	Drug delivery	Interactions with fluorescent unilamellar vesicles and dye-loaded mesoporous silica nanoparticles. Time-resolved fluorescence and steady-state techniques to study live cells fluorescence imaging. Release of dye molecules from the pores of mesoporous silica nanoparticles is observed (Bardhan et al. 2018)
Hollow-core mesoporous shell carbon nanospheres	Supercapacitor	Uniform hollow-core mesoporous shell carbon nanospheres fabricated by a surface co-assembly of monodisperse silica nanospheres method. This strategy is easier compared to other methods. 2.0 M sulfuric acid solution as the electrolyte: working electrode is hollow-core mesoporous shell carbon nanospheres coated glass carbon electrode, platinum electrode used as a counter. Good sustainability of capacitance (You et al. 2011)

2016). Results showed better selectivity and lower detection limit than graphene oxide without enclosed silica.

## Bioimaging

Silica nanoparticles can be easily utilized for molecular imaging techniques, such as optical imaging, e.g., fluorescence and bioluminescence, magnetic resonance imaging (MRI), radionuclide imaging, e.g., positron emission tomography (PET) and single-photon emission computed tomography (SPECT), computed tomography (CT), ultrasound, photoacoustic imaging and Raman imaging (Tang and Cheng 2013). Silica nanoparticles are used as contrast agents in medical imaging to encapsulate contrast agent particles such as an iron oxide (Lee et al. 2009), gold (Viabitskaya et al.

2011), silver (Gong et al. 2007), organic dyes (Yuan et al. 2005) and quantum dots (Hagura et al. 2011).

The 20–30 nm silica-coated fluorophore is photostable, and brightness is 20 times higher than composing fluorophores (Ow et al. 2005). The outer silica shell allows target specific cells and tissues by silica surface functionalization (Ow et al. 2005). Computed tomography is mostly used in diagnosis due to the limited depth of tissue penetration (Liu et al. 2012). A hybrid of silica with gold nanoparticles and fluorescein isothiocyanate dyes display a strong fluorescence signal at 520 nm under 490 nm excitation (Feng et al. 2014).

Silica-coated gold nanospheres can be coated with fluorescent quantum dots, yet further coating with silica is needed to reduce the defects of quantum dots (Song et al. 2015). This composite was used for contrast-enhanced computed tomography and fluorescence imaging. The probe of



in vivo gastric cancer cells using folic acid-conjugated silica coated with gold nanoclusters of about 58 nm size was used for computed tomography and fluorescence imaging (Zhou et al. 2013). Magnetic resonance imaging is mostly used for noninvasive diagnostic techniques (Viswanathan et al. 2010). Silica-coated gadolinium nanoparticles co-doped with europium ( $\text{Eu}^{3+}$ ) and terbium ( $\text{Tb}^{3+}$ ) were used for magnetic resonance and fluorescence imaging. Gadolinium carbonate particles are often used in magnetic resonance imaging. To increase biocompatibility, biomass-derived silica nanoparticles were conjugated with a fluorescent material and used for biological imaging application (Pandey et al. 2014). Here, meso-silica nanoparticles derived from rice husk were composited with green fluorescent carbon dots by hot injection. The complex shows high drug loading efficiency and stronger fluorescence compared to carbon dots alone. Thus, this complex material can be used for theranostic applications. Rice husk-derived silica composite with rare earth elements, europium/gadolinium ions were prepared by microwave-assisted combustion (Araichimani et al. 2020). Europium ions and gadolinium ions in the silica matrix exhibited potential of fluorescence imaging and T1-weighted magnetic resonance imaging, respectively. Thus, rice husk silica nanoparticles with rare earth ions are a good alternative for developing cost-effective bioimaging contrast agents.

## Drug delivery

Drug delivery systems based on silica nanoparticles are fast-developing in nanomedicine, yet it requires the analysis of toxicity, biodistribution, clearance and immune response of silica and modified silica (Biju 2014). Mesoporous silica nanoparticles are widely used for drug delivery application (Chowdhury 2018). Owing to the presence of surface silanol groups, they can be functionalized to tune the load and release of drugs (Vallet-Regí et al. 2007). Amine-functionalized mesoporous silica nanoparticles are widely used (Vallet-Regí et al. 2011). High drug loading and slow drug release are observed (Chowdhury, 2016). A such approach has been used for various drugs, e.g., heparin (Wan et al. 2012), hydrocortisone (Lopez et al. 2009), metoprolol (Guo et al. 2010), salidroside (Peng et al. 2013), venlafaxine (Tang et al. 2011), vancomycin (Lai et al. 2003), methotrexate (Carino et al. 2007), sophoridine (Dong et al. 2014) insulin and cyclic adenosine monophosphate (cAMP, Zhao et al. 2010), and anticancer drugs such as doxorubicin and 5-fluorouracil (Singh et al. 2011b; Mei et al. 2012; Wu et al. 2013a, b; Hwang et al. 2015).

Magnetic carbon nanotubes composited with mesoporous silica shows a high loading capacity for therapeutic molecules such as protein cytochrome C and drug gentamicin (Singh et al. 2014b). Small interfering RNA (siRNA) was

loaded and then released over a days to a week. Transferrin was grafted on the surfaces of mesoporous silica nanoparticles by a redox-cleavable disulfide bond, then was used as capping agent and targeting ligand (Chen et al. 2017). To examine the redox-responsive and burst release of doxorubicin, transferrin was integrated into mesoporous silica nanoparticles with the presence and absence of glutathione. Here, the presence of glutathione has perfect capping efficiency of transferrin and also enhanced the biocompatibility.

Nanocarriers of amine-modified mesoporous silica-iron oxide functionalized with 2, 3-dimercaptosuccinic acid via chemical amidation show that a negligible amount of the drug is released in the absence of a magnetic field (Chen et al. 2011). Upon application of a magnetic field, nanocaps are removed by chemical bond breaking, which induces high drug release. This material is also applicable for molecular imaging by T<sub>2</sub>-weighted magnetic resonance contrast influencing agents. Composites of rice husk-derived silica nanoparticles and polycaprolactone nanofibers are used for drug delivery of drugs such as allantoin (Ke et al. 2016). To reduce cost and increase biocompatibility, 5-fluorouracil was fixed to chitosan-coated biomass silica nanoparticles (Dhinasekaran et al. 2020). The results showed that potential in targeting the cancer cell lines MCF-7 and A549.

## Supercapacitors

Supercapacitors have attracted interest owing to their extended cycle life performance, high charge/discharge rates and high power density (Miller and Simon 2008; Liu et al. 2010; Simon and Gogotsi 2010). Supercapacitors are considered as a very promising energy storage device to complement or eventually replace the batteries of wearable and portable electronics, and electrical and hybrid vehicles (Kaempgen et al. 2009). Supercapacitors can be classified into two main categories according to the energy storage mechanisms: electric double-layer capacitors (EDLC) and pseudocapacitors (Winter and Brodd 2004). Mesoporous silica nanoparticles with conducting polyaniline wires wrapped with graphene oxide were found to expand the surface area and allow the movement of ions and charge transfer (Javed et al. 2018).

Manganese dioxide/mesoporous nanocomposite are obtained by facile chemical synthesis and then used as electrode material for supercapacitor applications, thus displayed superior electrochemical performance (Huang et al. 2017). Rice-derived silicon was composited with carbon ( $\text{SiO}_x/\text{C}$ ) for Li-ion batteries by one-step pyrolysis exhibiting  $\text{SiO}_x/\text{C}$  anode specific capacity of 654 mAh g<sup>-1</sup> after 1000 cycles, with higher capacity up to 920 mAh g<sup>-1</sup> (Huang et al. 2019). To use rice husk for energy storage, tin oxide was decorated on husk-derived silica nanoparticles by facile microwave combustion

(Vijayan et al. 2020). Here, the presence tin oxide on silica nanosphere provides reactive surfaces for charges adsorption and desorption.

Silica nanoparticles are not only used in the biomedical field but also used in various fields such as material packing, textile (Riaz et al. 2019), agriculture and food (Rastogi et al. 2019), adsorbents in the removal of organic and inorganic pollutants (Morin-Crini et al. 2019), rubber field (Peng et al. 2007), water treatment (Demadis and Mavredaki 2005), concrete and construction and photocatalytic degradation (Alaoui et al. 2009 and Batista et al. 2010).

## Conclusion

Silica nanoparticles are promising material for medical and electronics applications. Because of its optoelectronic properties, silicon (Si) is extensively used in photovoltaic and energy storage applications. Recently, the application of silica is also explored in biomedical fields in the form of silica nanoparticles as bioimaging, biosensors and drug delivery, due to its biocompatibility, biodegradability and low toxicity. The silica nanoparticles can be prepared by different methods and most of the researchers used the well-known Stober method to get monodispersed particles with narrow size distribution. Compared to silica nanoparticles prepared using tetraethylorthosilicate as a precursor, silica nanoparticles from biomass are exhibiting good properties at low cost. Silica sources can also be obtainable from rice husk, sugarcane bagasse, corn cob and wheat husk.

**Acknowledgement** D. Durgalakshmi gratefully acknowledges the Department of Science & Technology (DST) Innovation in Science Pursuit for Inspired Research (INSPIRE) under Faculty scheme (DST/INSPIRE/04/2016/000845), New Delhi.

## References

- Adesanya D, Raheem A (2009) Development of corn cob ash blended cement. *Constr Build Mater* 23(1):347–352. <https://doi.org/10.1016/j.conbuildmat.2007.11.013>
- Aigbodion V, Hassan S, Ause T, Nyior G (2010) Potential utilization of solid waste (bagasse ash). *J Minerals Mater Characterization Eng* 9(01):67. <https://doi.org/10.4236/jmmce.2010.91006>
- Ajayi B, Owoeye S (2015) Extraction of soluble sodium silicate using corn cob ash as a silica source. *Am J Eng Res* 4(9):54–56
- Alaoui OT, Nguyen QT, Rhlalou TJECL (2009) Preparation and characterization of a new TiO<sub>2</sub>/SiO<sub>2</sub> composite catalyst for photocatalytic degradation of indigo carmin. *Environ Chem Lett* 7(2):175–181. <https://doi.org/10.1007/s10311-008-0154-1>
- Al-Ogaidi I, Gou H, Al-Kazaz AKA, Aguilar ZP, Melconian AK, Zheng P, Wu N (2014) A gold@ silica core-shell nanoparticle-based surface-enhanced Raman scattering biosensor for label-free glucose detection. *Anal Chim Acta* 811:76–80. <https://doi.org/10.1016/j.aca.2013.12.009>
- Amiri M, Salavati-Niasari M, Akbari A (2017) A magnetic CoFe<sub>2</sub>O<sub>4</sub>/SiO<sub>2</sub> nanocomposite fabricated by the sol-gel method for electrocatalytic oxidation and determination of L-cysteine. *Microchim Acta* 184(3):825–833. <https://doi.org/10.1007/s00604-016-2064-4>
- Araichimani P, Prabu K, Kumar GS, Karunakaran G, Van Minh N, Karthi S, Girija E, Kolesnikov E (2020) Rare-earth ions integrated silica nanoparticles derived from rice husk via microwave-assisted combustion method for bioimaging applications. *Ceram Int* 46(11):18366–18372. <https://doi.org/10.1016/j.ceramint.2020.04.125>
- Aribo S (2011) Effect of varying corn cob and rice husk ashes on properties of moulding sand. *J Minerals Mater Characterization Eng* 10(15):1449. <https://doi.org/10.4236/jmmce.2011.1015112>
- Ariffin EY, Lee YH, Futra D, Tan LL, Karim NHA, Ibrahim NNN, Ahmad A (2018) An ultrasensitive hollow-silica-based biosensor for pathogenic Escherichia coli DNA detection. *Anal Bioanal Chem* 410(9):2363–2375. <https://doi.org/10.1007/s00216-018-0893-1>
- Atabaev TS, Lee JH, Han D-W, Choo KS, Jeon UB, Hwang JY, Yeom JA, Kang C, Kim H-K, Hwang Y-H (2016) Multicolor nanoparticles based on silica-coated gadolinium oxide nanoparticles with highly reduced toxicity. *RSC Adv* 6(24):19758–19762. <https://doi.org/10.1039/c5ra27685c>
- Athinarayanan J, Periasamy VS, Alhazmi M, Alshatwi AA (2017) Synthesis and biocompatibility assessment of sugarcane bagasse-derived biogenic silica nanoparticles for biomedical applications. *J Biomed Mater Res B Appl Biomater* 105(2):340–349. <https://doi.org/10.1002/jbm.b.33511>
- Azlina H, Hasnidawani J, Norita H, Surip S (2016) Synthesis of SiO<sub>2</sub> nanostructures using sol-gel method. *Acta Phys Pol A* 129(4):842–844. <https://doi.org/10.12693/aphyspola.129.842>
- Azmi M, Ismail N, Rizamarhaiza M, Taib H (2016) Characterisation of silica derived from rice husk (Muar, Johor, Malaysia) decomposition at different temperatures, AIP Conference Proceedings. AIP Publishing, College Park. <https://doi.org/10.1063/1.4958748>
- Babaso PN, Sharanagouda H (2017) Rice husk and its applications. *Int J Curr Microbiol Appl Sci* 6(10):1144–1156. <https://doi.org/10.20546/ijcmas.2017.610.138>
- Bae SW, Tan W, Hong J-I (2012) Fluorescent dye-doped silica nanoparticles: new tools for bioapplications. *Chem Commun* 48(17):2270–2282. <https://doi.org/10.1039/c2cc16306c>
- Bai Y, Yang H, Yang W, Li Y, Sun C (2007) Gold nanoparticles-mesoporous silica composite used as an enzyme immobilization matrix for amperometric glucose biosensor construction. *Sensors Actuators B Chem* 124(1):179–186. <https://doi.org/10.1016/j.snb.2006.12.020>
- Balagna C, Perero S, Percivalle E, Nepita EV, Ferraris M (2020) Virucidal effect against coronavirus SARS-CoV-2 of a silver nanocluster/silica composite sputtered coating. *Open Ceram* 1:100006. <https://doi.org/10.1016/j.oceram.2020.100006>
- Bardhan M, Majumdar A, Jana S, Ghosh T, Pal U, Swarnakar S, Senapati D (2018) Mesoporous silica for drug delivery: Interactions with model fluorescent lipid vesicles and live cells. *J Photochem Photobiol B* 178:19–26. <https://doi.org/10.1016/j.jphotobiol.2017.10.023>
- Barrabino A (2011) Synthesis of mesoporous silica particles with control of both pore diameter and particle size. Master's thesis
- Batista AP, Carvalho HWP, Luz GH, Martins PF, Gonçalves M, Oliveira LCJECL (2010) Preparation of CuO/SiO<sub>2</sub> and photocatalytic activity by degradation of methylene blue. *Environ Chem Lett* 8(1):63–67. <https://doi.org/10.1007/s10311-008-0192-8>
- Beck JS, Vartuli J, Roth WJ, Leonowicz M, Kresge C, Schmitt K, Chu C, Olson DH, Sheppard E, McCullen S (1992) A new family of mesoporous molecular sieves prepared with liquid crystal templates. *J Am Chem Soc* 114(27):10834–10843. <https://doi.org/10.1021/ja00053a020>

- Beganskienė A, Sirutkaitis V, Kurtinaitienė M, Juškėnas R, Kareiva A (2004) FTIR, TEM and NMR investigations of Stöber silica nanoparticles. *Mater Sci (Medžiagotyra)* 10:287–290
- Bell R, Bird N, Dean P (1968) The vibrational spectra of vitreous silica, germania and beryllium fluoride. *J Phys C Solid State Phys* 1(2):299. <https://doi.org/10.1088/0022-3719/1/2/304>
- Bharti C, Nagaich U, Pal AK, Gulati N (2015) Mesoporous silica nanoparticles in target drug delivery system: a review. *Int J Pharmaceutical Investigation* 5(3):124. <https://doi.org/10.4103/2230-973x.160844>
- Biju V (2014) Chemical modifications and bioconjugate reactions of nanomaterials for sensing, imaging, drug delivery and therapy. *Chem Soc Rev* 43(3):744–764. <https://doi.org/10.1039/c3cs60273g>
- Bhuvaneshwari S, Hettiarachchi H, Meegoda JN (2019) Crop residue burning in India: policy challenges and potential solutions. *Int J Environ Res Public Health* 16(5):832. <https://doi.org/10.3390/ijerph16050832>
- Bleta R, Ponchel A, Monflier E (2018) Cyclodextrin-based supramolecular assemblies: a versatile toolbox for the preparation of functional porous materials. *Environ Chem Lett* 16:1393–1413. <https://doi.org/10.1007/s10311-018-0768-x>
- Bogush G, Tracy M, Zukoski Iv C (1988) Preparation of monodisperse silica particles: control of size and mass fraction. *J Non-Cryst Solids* 104(1):95–106. [https://doi.org/10.1016/0022-3093\(88\)90187-1](https://doi.org/10.1016/0022-3093(88)90187-1)
- Bosio A, Rodella N, Gianoncelli A, Zacco A, Borgese L, Depero L, Bingham P, Bontempi EJEcl (2013) A new method to inertize incinerator toxic fly ash with silica from rice husk ash. *Environ Chem Lett* 11(4):329–333. <https://doi.org/10.1007/s10311-013-0411-9>
- Brinker CJ, Scherer GW (2013) Sol-gel science: the physics and chemistry of sol-gel processing. Academic Press, New York
- Burda C, Chen X, Narayanan R, El-Sayed MA (2005) Chemistry and properties of nanocrystals of different shapes. *Chem Rev* 105(4):1025–1102. <https://doi.org/10.1021/cr030063a>
- Cai Q, Luo Z-S, Pang W-Q, Fan Y-W, Chen X-H, Cui F-Z (2001) Dilute solution routes to various controllable morphologies of MCM-41 silica with a basic medium. *Chem Mater* 13(2):258–263. <https://doi.org/10.1021/cm990661z>
- Caras A (2011) Glucan particle delivery of mesoporous silica-drug nanoparticles. UMASS Medical School. <https://doi.org/10.1155/2012/143524>
- Carino IS, Pasqua L, Testa F, Aiello R, Puoci F, Iemma F, Picci N (2007) Silica-based mesoporous materials as drug delivery system for methotrexate release. *Drug Delivery* 14(8):491–495. <https://doi.org/10.1080/10717540701606244>
- Carmona V, Oliveira R, Silva W, Mattoso L, Marconcini J (2013) Nanosilica from rice husk: extraction and characterization. *Ind Crops Prod* 43:291–296. <https://doi.org/10.1016/j.indcrop.2012.06.050>
- Carrasco S, Benito-Peña E, Navarro-Villoslada F, Langer J, Sanz-Ortiz MN, Reguera J, Moreno-Bondi L-M, MCJCoM, (2016) Multibranched gold–mesoporous silica nanoparticles coated with a molecularly imprinted polymer for label-free antibiotic surface-enhanced Raman scattering analysis. *Chem Mater* 28(21):7947–7954. <https://doi.org/10.1021/acs.chemmater.6b03613>
- Chandrasekhar S, Satyanarayana K, Pramada P, Raghavan P, Gupta T (2003) Review processing, properties and applications of reactive silica from rice husk—an overview. *J Mater Sci* 38(15):3159–3168. <https://doi.org/10.1023/a:1025157114800>
- Chatterjee K, Sarkar S, Rao KJ, Paria S (2014) Core/shell nanoparticles in biomedical applications. *Adv Coll Interface Sci* 209:8–39. <https://doi.org/10.1016/j.cis.2013.12.008>
- Chaubey A, Malhotra B (2002) Mediated biosensors. *Biosens Bioelectron* 17(6–7):441–456
- Chen M, Xia L, Xue P (2007) Enzymatic hydrolysis of corncob and ethanol production from cellulosic hydrolysate. *Int Biodeterior Biodegradation* 59(2):85–89. <https://doi.org/10.1016/j.ibiod.2006.07.011>
- Chen P-J, Hu S-H, Hsiao C-S, Chen Y-Y, Liu D-M, Chen S-Y (2011) Multifunctional magnetically removable nanogated lids of Fe<sub>3</sub>O<sub>4</sub>-capped mesoporous silica nanoparticles for intracellular controlled release and MR imaging. *J Mater Chem* 21(8):2535–2543. <https://doi.org/10.1039/c0jm02590a>
- Chen S, Wang L, Duce SL, Brown S, Lee S, Melzer A, Cuschieri SA, André P (2010) Engineered biocompatible nanoparticles for in vivo imaging applications. *J Am Chem Soc* 132(42):15022–15029. <https://doi.org/10.1021/ja106543j>
- Chen X, Sun H, Hu J, Han X, Liu H, Hu Y (2017) Transferrin gated mesoporous silica nanoparticles for redox-responsive and targeted drug delivery. *Colloids Surf B* 152:77–84. <https://doi.org/10.1016/j.colsurfb.2017.01.010>
- Chen Z, Tan Y, Xu K, Zhang L, Qiu B, Guo L, Lin Z, Chen G (2016) Stimulus-response mesoporous silica nanoparticle-based chemiluminescence biosensor for cocaine determination. *Biosens Bioelectron* 75:8–14. <https://doi.org/10.1016/j.bios.2015.08.006>
- Chowdhury MA (2016) The controlled release of drugs and bioactive compounds from mesoporous silica nanoparticles. *Curr Drug Deliv* 13(6):839–856. <https://doi.org/10.2174/1567201813666151202195104>
- Chowdhury MA (2018) Silica materials for biomedical applications in drug delivery, bone treatment or regeneration, and MRI contrast agent. *Rev J Chem* 8(2):223–241. <https://doi.org/10.1134/s2079978018020024>
- Chusilp N, Jaturapitakkul C, Kiattikomol K (2009) Effects of LOI of ground bagasse ash on the compressive strength and sulfate resistance of mortars. *Constr Build Mater* 23(12):3523–3531. <https://doi.org/10.1016/j.conbuildmat.2009.06.046>
- Corr SA, Rakovich YP, Gun'ko YK (2008) Multifunctional magnetic-fluorescent nanocomposites for biomedical applications. *Nanoscale Res Lett* 3(3):87. <https://doi.org/10.1007/s11671-008-9122-8>
- Croissant JG, Guardado-Alvarez TMJI (2019) Photocracking silica: tuning the plasmonic photothermal degradation of mesoporous silica encapsulating gold nanoparticles for Cargo release. *Inorganics* 7(6):72. <https://doi.org/10.3390/inorganics7060072>
- Dabbaghian M, Babalou A, Hadi P, Jannatdoust E (2010) A parametric study of the synthesis of silica nanoparticles via sol-gel precipitation method. *Int J Nanosci Nanotechnol* 6(2):104–113
- De Souza M, Magalhães W, Persegil M (2002) Silica derived from burned rice hulls. *Mater Res* 5(4):467–474. <https://doi.org/10.1590/s1516-14392002000400012>
- Della VP, Kühn I, Hotza D (2002) Rice husk ash as an alternate source for active silica production. *Mater Lett* 57(4):818–821. [https://doi.org/10.1016/s0167-577x\(02\)00879-0](https://doi.org/10.1016/s0167-577x(02)00879-0)
- Demadis KD, Mavredaki EJECL (2005) Green additives to enhance silica dissolution during water treatment. *Environ Chem Lett* 3(3):127–131. <https://doi.org/10.1007/s10311-005-0015-0>
- Devi MG, Balachandran S (2016) A review on synthesis, characterization and applications of silica particles international journal of advanced. *Eng Technol* 4:249–255
- Devine RA, Durand J-P, Dooryhée E (2000) Structure and imperfections in amorphous and crystalline silicon dioxide. Wiley, New York
- Ding X, Zhao J, Liu Y, Zhang H, Wang Z (2004) Silica nanoparticles encapsulated by polystyrene via surface grafting and in situ emulsion polymerization. *Mater Lett* 58(25):3126–3130. <https://doi.org/10.1016/j.matlet.2004.06.003>

- Dong L, Peng H, Wang S, Zhang Z, Li J, Ai F, Zhao Q, Luo M, Xiong H, Chen L (2014) Thermally and magnetically dual-responsive mesoporous silica nanospheres: preparation, characterization, and properties for the controlled release of sophoridine. *J Appl Polymer Sci* 131(13). <https://doi.org/10.1002/app.40477>
- Douglas BE, Ho S-M (2006) Crystal structures of silica and metal silicates. *Struct Chem Crystalline Solids*, 233–278. [https://doi.org/10.1007/0-387-36687-3\\_10](https://doi.org/10.1007/0-387-36687-3_10)
- Dubey R, Rajesh Y, More M (2015) Synthesis and characterization of SiO<sub>2</sub> nanoparticles via sol-gel method for industrial applications. *Mater Today Proc* 2(4–5):3575–3579. <https://doi.org/10.1016/j.matpr.2015.07.098>
- Dhinasekaran D, Raj R, Rajendran AR, Purushothaman B, Subramanian B, Prakasarao A, Singaravelu G (2020) Chitosan mediated 5-Fluorouracil functionalized silica nanoparticle from rice husk for anticancer activity. *Int J Biol Macromol* 156:969–980. <https://doi.org/10.1016/j.ijbiomac.2020.04.098>
- Eurov DA, Kurdyukov DA, Kirilenko DA, Kukushkina JA, Nashchekin AV, Smirnov AN, Golubev VG (2015) Core-shell monodisperse spherical mSiO<sub>2</sub>/Gd<sub>2</sub>O<sub>3</sub>:Eu<sup>3+</sup>@mSiO<sub>2</sub> particles as potential multifunctional theranostic agents. *J Nanopart Res* 17(2):82. <https://doi.org/10.1007/s11051-015-2891-y>
- Fanderlik I (2013) Silica glass and its application. Elsevier, Amsterdam
- Fardad M (2000) Catalysts and the structure of SiO<sub>2</sub> sol-gel films. *J Mater Sci* 35(7):1835–1841. <https://doi.org/10.1023/A:1004749107134>
- Faria K, Gurgel R, Holanda J (2012) Recycling of sugarcane bagasse ash waste in the production of clay bricks. *J Environ Manage* 101:7–12. <https://doi.org/10.1016/j.jenvman.2012.01.032>
- Feng J, Chang D, Wang Z, Shen B, Yang J, Jiang Y, Ju S, He N (2014) A FITC-doped silica coated gold nanocomposite for both in vivo X-ray CT and fluorescence dual modal imaging. *RSC Adv* 4(94):51950–51959. <https://doi.org/10.1039/c4ra09392e>
- Feng Q, Chen K, Ma D, Lin H, Liu Z, Qin S, Luo Y (2018) Synthesis of high specific surface area silica aerogel from rice husk ash via ambient pressure drying. *Colloids Surf A* 539:399–406. <https://doi.org/10.1016/j.colsurfa.2017.12.025>
- Finnie KS, Bartlett JR, Barbé CJ, Kong LJJ (2007) Formation of silica nanoparticles in microemulsions. *Langmuir* 23(6):3017–3024. <https://doi.org/10.1021/la0624283>
- Ganesan K, Rajagopal K, Thangavel K (2007) Evaluation of bagasse ash as supplementary cementitious material. *Cement Concr Compos* 29(6):515–524. <https://doi.org/10.1016/j.cemconcomp.2007.03.001>
- Geetha D, Ananthiand A, Ramesh P (2016) Preparation and characterization of silica material from rice husk ash—an economically viable method. *Res Rev J Pure Appl Phys* 4(3):20–26
- Gelperina S, Kisich K, Iseman MD, Heifets L (2005) The potential advantages of nanoparticle drug delivery systems in chemotherapy of tuberculosis. *Am J Respir Crit Care Med* 172(12):1487–1490
- Gerber T, Himmel B (1986) The structure of silica glass. *J Non-Cryst Solids* 83(3):324–334. [https://doi.org/10.1016/0022-3093\(86\)90245-0](https://doi.org/10.1016/0022-3093(86)90245-0)
- Giddel M, Jivan A (2007) Waste to wealth, potential of rice husk in India a literature review, International conference on cleaner technologies and environmental Management PEC, Pondicherry, India
- Gilmore JL, Yi X, Quan L, Kabanov AV (2008) Novel nanomaterials for clinical neuroscience. *J NeuroImmune Pharmacol* 3(2):83–94. <https://doi.org/10.1007/s11481-007-9099-6>
- Gong J-L, Liang Y, Huang Y, Chen J-W, Jiang J-H, Shen G-L, Yu R-Q (2007) Ag/SiO<sub>2</sub> core-shell nanoparticle-based surface-enhanced Raman probes for immunoassay of cancer marker using silica-coated magnetic nanoparticles as separation tools. *Biosens Bioelectron* 22(7):1501–1507. <https://doi.org/10.1016/j.bios.2006.07.004>
- Goyal A, Kunio H, Hidehiko O (2007) Mandula. Properties and Reactivity of Sugarcane Bagasse Ash, Tottori University, Japan
- Greasley SL, Page SJ, Sirovica S, Chen S, Martin RA, Riveiro A, Hanna JV, Porter AE, Jones JR (2016) Controlling particle size in the Stöber process and incorporation of calcium. *J Colloid Interface Sci* 469:213–223. <https://doi.org/10.1016/j.jcis.2016.01.065>
- Greenwood N, Earnshaw A (1997) Chemistry of the elements, 2nd edn. Butterworth-Heinemann, Oxford. <https://doi.org/10.1016/b978-0-7506-3365-9.50005-5>
- Grün M, Lauer I, Unger KK (1997) The synthesis of micrometer- and submicrometer-size spheres of ordered mesoporous oxide MCM-41. *Adv Mater* 9(3):254–257. <https://doi.org/10.1002/adma.19970090317>
- Gu L, Zhang A, Hou K, Dai C, Zhang S, Liu M, Song C, Guo XJM, Materials M (2012) One-pot hydrothermal synthesis of mesoporous silica nanoparticles using formaldehyde as growth suppressant. *Microporous Mesoporous Mater* 152:9–15. <https://doi.org/10.1016/j.micromeso.2011.11.047>
- Guo Q, Huang D, Kou X, Cao W, Li L, Ge L, Li J (2017) Synthesis of disperse amorphous SiO<sub>2</sub> nanoparticles via sol-gel process. *Ceram Int* 43(1):192–196. <https://doi.org/10.1016/j.ceramint.2016.09.133>
- Guo Z, Du Y, Liu X, Ng S-C, Chen Y, Yang Y (2010) Enantioselectively controlled release of chiral drug (metoprolol) using chiral mesoporous silica materials. *Nanotechnology* 21(16):165103. <https://doi.org/10.1088/0957-4484/21/16/165103>
- Hagura N, Ogi T, Shirahama T, Iskandar F, Okuyama K (2011) Highly luminescent silica-coated ZnO nanoparticles dispersed in an aqueous medium. *J Lumin* 131(5):921–925. <https://doi.org/10.1016/j.jlumin.2010.12.024>
- Hajarul AAW, Nor DZ, Aziz AA, Khairunisak AR (2011) Properties of amorphous silica entrapped isoniazid drug delivery system. *Adv Mater Res* 364:134–138
- Hariharan V, Sivakumar G (2013) Studies on synthesized nanosilica obtained from bagasse ash. *Int J Chem Tech Res* 5(3):1263–1266
- Henderson G, Baker DR (2002) Synchrotron radiation: earth, environmental and materials sciences applications. <https://doi.org/10.1007/s00126-002-0329-9>
- Hoffmann F, Cornelius M, Morell J, Fröba M (2006) Silica-based mesoporous organic-inorganic hybrid materials. *Angew Chem Int Ed* 45(20):3216–3251. <https://doi.org/10.1002/anie.200503075>
- Holden NE (2001) History of the origin of the chemical elements and their discoverers. Prepared for the 41st IUPAC General Assembly 29. <https://doi.org/10.1515/ci.2001.23.5.129>
- Hossain SS, Mathur L, Roy P (2018) Rice husk/rice husk ash as an alternative source of silica in ceramics: a review. *J Asian Ceram Soc* 6(4):299–313. <https://doi.org/10.1080/21870764.2018.1539210>
- Hu J, Wang W, Yu R, Guo M, He C, Xie X, Peng H, Xue Z (2017) Solid polymer electrolyte based on ionic bond or covalent bond functionalized silica nanoparticles. *RSC Adv* 7(87):54986–54994. <https://doi.org/10.1039/c7ra08471d>
- Hu W-Y, Liu H, Shao Y-Z (2015) Fluorescein isothiocyanate embedded silica spheres in gadolinium carbonate shells as novel magnetic resonance imaging and fluorescence bi-modal contrast agents. *New J Chem* 39(9):7363–7371. <https://doi.org/10.1039/c5nj00537j>
- Huabcharoen P, Wimolmala E, Markpin T, Sombatsompop N (2017) Purification and characterization of silica from sugarcane Bagasse ash as a reinforcing filler in natural rubber composites. *BioResources* 12(1):1228–1245. <https://doi.org/10.15376/biores.12.1.1228-1245>

- Huang HS, Chang KH, Suzuki N, Yamauchi Y, Hu CC, Wu KCW (2013) Evaporation-induced coating of hydrous Ruthenium oxide on mesoporous silica nanoparticles to develop high-performance supercapacitors. *Small* 9(15):2520–2526. <https://doi.org/10.1002/smll.201202786>
- Huang Q, Lin X, Lin C, Zhang Y, Hu S, Wei C (2015) A high performance electrochemical biosensor based on Cu<sub>2</sub>O-carbon dots for selective and sensitive determination of dopamine in human serum. *RSC Adv* 5(67):54102–54108. <https://doi.org/10.1039/c5ra05433h>
- Huang Y, Li SFY (2013) Electrocatalytic performance of silica nanoparticles on graphene oxide sheets for hydrogen peroxide sensing. *J Electroanal Chem* 690:8–12. <https://doi.org/10.1016/j.jelechem.2012.11.041>
- Huang Y, Weng D, Han L, Wang Y, Liu K, Yan J, Lu J (2017) Synthesis and characterization of MnO<sub>2</sub>/Hollow mesoporous silica nanocomposite as electrode materials for application in supercapacitors. *Nanosci Nanotechnol Lett* 9(11):1639–1648. <https://doi.org/10.1166/nml.2017.2534>
- Huang S-S, Tung MT, Huynh CD, Hwang B-J, Bieker PM, Fang C-C, Wu N-L (2019) Engineering rice husk into a high-performance electrode material through an ecofriendly process and assessing its application for lithium-ion sulfur batteries. *ACS Sustain Chem Eng* 7(8):7851–7861. <https://doi.org/10.1021/acssuschemeng.9b00092>
- Hui N, Wang S, Xie H, Xu S, Niu S, Luo X (2015) Nickel nanoparticles modified conducting polymer composite of reduced graphene oxide doped poly (3, 4-ethylenedioxythiophene) for enhanced nonenzymatic glucose sensing. *Sensors Actuators B Chem* 221:606–613. <https://doi.org/10.1016/j.snb.2015.07.011>
- Hwang AA, Lu J, Tamanoi F, Zink JI (2015) Functional nanovalves on protein-coated nanoparticles for in vitro and in vivo controlled drug delivery. *Small* 11(3):319–328. <https://doi.org/10.1002/smll.201400765>
- Ibrahim IA, Zikry A, Sharaf MA (2010) Preparation of spherical silica nanoparticles: Stober silica. *J Am Sci* 6(11):985–989
- Jang ES, Lee SY, Cha E-J, Sun I-C, Kwon IC, Kim D, Kim YI, Kim K, Ahn C-H (2014) Fluorescent dye labeled iron oxide/silica core/shell nanoparticle as a multimodal imaging probe. *Pharm Res* 31(12):3371–3378. <https://doi.org/10.1007/s11095-014-1426-z>
- Javed M, Abbas SM, Siddiq M, Han D, Niu L (2018) Mesoporous silica wrapped with graphene oxide-conducting PANI nanowires as a novel hybrid electrode for supercapacitor. *J Phys Chem Solids* 113:220–228. <https://doi.org/10.1016/j.jpcs.2017.10.037>
- Jin S-A, Poudyal S, Marinero EE, Kuhn RJ, Stanciu LA (2016) Impedimetric dengue biosensor based on functionalized graphene oxide wrapped silica particles. *Electrochim Acta* 194:422–430. <https://doi.org/10.1016/j.electacta.2016.02.116>
- Joshaghani A, Moeini MAJC, Materials B (2017) Evaluating the effects of sugar cane bagasse ash (SCBA) and nanosilica on the mechanical and durability properties of mortar. *Constr Build Mater* 152:818–831. <https://doi.org/10.1016/j.conbuildmat.2017.07.041>
- Ju J, Chen W (2015) In situ growth of surfactant-free gold nanoparticles on nitrogen-doped graphene quantum dots for electrochemical detection of hydrogen peroxide in biological environments. *Anal Chem* 87(3):1903–1910. <https://doi.org/10.1021/ac5041555>
- Kaempgen M, Chan CK, Ma J, Cui Y, Gruner G (2009) Printable thin film supercapacitors using single-walled carbon nanotubes. *Nano Lett* 9(5):1872–1876. <https://doi.org/10.1021/nl8038579>
- Kaliyan N, Morey RV (2010) Densification characteristics of corn cobs. *Fuel Process Technol* 91(5):559–565. <https://doi.org/10.1016/j.fuproc.2010.01.001>
- Ke M, Wahab JA, Hyunsik B, Song K-H, Lee JS, Gopiraman M, Kim IS (2016) Allantoin-loaded porous silica nanoparticles/polycaprolactone nanofiber composites: fabrication, characterization, and drug release properties. *RSC Advances* 6(6):4593–4600. <https://doi.org/10.1039/c5ra22199d>
- Kim TG, An GS, Han JS, Hur JU, Park BG, Choi S-C (2017) Synthesis of size controlled spherical silica nanoparticles via sol-gel process within hydrophilic solvent. *J Korean Ceram Soc* 54(1):49–54. <https://doi.org/10.4191/kcers.2017.54.1.10>
- Klabunde K (2001) Introduction to the nanoworld. *Nanoscale Mater Chem*, 6–7.
- Kobayashi Y, Imai J, Nagao D, Takeda M, Ohuchi N, Kasuya A, Konno M (2007) Preparation of multilayered silica-Gd-silica core-shell particles and their magnetic resonance images. *Colloids Surf A* 308(1–3):14–19. <https://doi.org/10.1016/j.colsurfa.2007.05.024>
- Kobayashi Y, Matsudo H, Li T-t, Shibuya K, Kubota Y, Oikawa T, Nakagawa T, Gonda K (2016) Fabrication of quantum dot/silica core-shell particles immobilizing Au nanoparticles and their dual imaging functions. *Appl Nanosci* 6(3):301–307. <https://doi.org/10.1007/s13204-015-0440-8>
- Koch EC, Clément D (2007) Special materials in pyrotechnics: VI. Silicon—an old fuel with new perspectives. *Propellants Explosives Pyrotechnics Int J Deal Sci Technol Asp Energetic Mater* 32(3):205–212. <https://doi.org/10.1002/prep.200700021>
- Korzhinsky M, Tkachenko S, Shmulovich K, Steinberg G (1995) Native Al and Si formation. *Nature* 375(6532):544. <https://doi.org/10.1038/375544a0>
- Kresge C, Leonowicz M, Roth WJ, Vartuli J, Beck J (1992) Ordered mesoporous molecular sieves synthesized by a liquid-crystal template mechanism. *nature* 359(6397), 710. [doi.org/https://doi.org/10.1038/359710a0](https://doi.org/10.1038/359710a0)
- Kumar S, Upadhyaya JS, Negi YS (2010) Preparation of nanoparticles from corn cobs by chemical treatment methods. *BioResources* 5(2):1292–1300
- Kuswandi BJECL (2019) Nanobiosensor approaches for pollutant monitoring. *Environ Chem Lett* 17(2):975–990. <https://doi.org/10.1007/s10311-018-00853-x>
- Lai C-Y, Trewyn BG, Jeftinija DM, Jeftinija K, Xu S, Jeftinija S, Lin VS-Y (2003) A mesoporous silica nanosphere-based carrier system with chemically removable CdS nanoparticle caps for stimuli-responsive controlled release of neurotransmitters and drug molecules. *J Am Chem Soc* 125(15):4451–4459. <https://doi.org/10.1021/ja0286501>
- Law W-C, Yong K-T, Roy I, Xu G, Ding H, Bergey EJ, Zeng H, Prasad PN (2008) Optically and magnetically doped organically modified silica nanoparticles as efficient magnetically guided biomarkers for two-photon imaging of live cancer cells. *The Journal of Physical Chemistry C* 112(21):7972–7977. <https://doi.org/10.1021/jp712090y>
- Lee K, Moon H-Y, Park C, Kim OR, Ahn E, Lee SY, Park HE, Ihm S-H, Seung K-B, Chang K (2009) Magnetic resonance imaging of macrophage activity in atherosclerotic plaques of apolipoprotein E-deficient mice by using polyethylene glycolated magnetic fluorescent silica-coated nanoparticles. *Curr Appl Phys* 9(1):S15–S18. <https://doi.org/10.1016/j.cap.2008.08.040>
- Lieberman A, Mendez N, Trogler WC, Kummel AC (2014) Synthesis and surface functionalization of silica nanoparticles for nanomedicine. *Surf Sci Rep* 69(2):132–158. <https://doi.org/10.1016/j.surfrep.2014.07.001>
- Lichtfouse E, Rullkötter J (1994) Accelerated transformation of organic matter below the silica transition zone in immature sediments from the Japan Sea. *Org Geochem* 21:517–523. [https://doi.org/10.1016/0146-6380\(94\)90102-3](https://doi.org/10.1016/0146-6380(94)90102-3)
- Lide DR (2004) Handbook of chemistry and physics, 85th edn. CRC, Boca Raton, pp 186–187
- Liou T-H, Yang C-C (2011) Synthesis and surface characteristics of nanosilica produced from alkali-extracted rice husk ash.

- Mater Sci Eng B 176(7):521–529. <https://doi.org/10.1016/j.mseb.2011.01.007>
- Liu C, Li F, Ma LP, Cheng HM (2010) Advanced materials for energy storage. *Adv Mater* 22(8):E28–E62
- Liu X, Chen X, Yang L, Chen H, Tian Y, Wang Z (2016) A review on recent advances in the comprehensive application of rice husk ash. *Res Chem Intermed* 42(2):893–913. <https://doi.org/10.1007/s11164-015-2061-y>
- Liu Y, Ai K, Lu L (2012) Nanoparticulate X-ray computed tomography contrast agents: from design validation to in vivo applications. *Acc Chem Res* 45(10):1817–1827. <https://doi.org/10.1002/adma.200903328>
- Liu Y, Chen S-S, Wang A-J, Feng J-J, Wu X, Weng X (2016) An ultrasensitive electrochemical sensor for hydrazine based on AuPd nanorod alloy nanochains. *Electrochim Acta* 195:68–76. <https://doi.org/10.1016/j.electacta.2016.01.229>
- Lopez T, Ortiz E, Alexander-Katz R, Basaldella E, Bokhimi X (2009) Cortisol controlled release by mesoporous silica. *Nanomed Nanotechnol Biol Med* 5 (2), 170–177. <https://doi.org/10.1016/j.nano.2008.08.002>
- Lunevich L, Sanciolo P, Smallridge A, Gray S (2016) Silica scale formation and effect of sodium and aluminium ions-29 Si NMR study. *Environ Sci Water Res Technol* 2(1):174–185. <https://doi.org/10.1039/c5ew00220f>
- Luo X, Cao JJECL (2018) Discovery of nano-sized gold particles in natural plant tissues. *Environ Chem Lett* 16(4):1441–1448. <https://doi.org/10.1007/s10311-018-0749-0>
- Madrid R, Nogueira C, Margarido F (2012) Production and characterisation of amorphous silica from rice husk waste, *WasteEng' 2012*. In: Proceedings of the 4th international conference on engineering for waste and biomass valorisation 2012
- Mahajan A, Gupta P (2020) Carbon-based solid acids: a review. *Environ Chem Lett* 18:299–314. <https://doi.org/10.1007/s10311-019-00940-7>
- Mandal A, Chakrabarty D (2011) Isolation of nanocellulose from waste sugarcane bagasse (SCB) and its characterization. *Carbohydr Polym* 86(3):1291–1299. <https://doi.org/10.1016/j.carbpol.2011.06.030>
- Manzano M, Aina V, Arean C, Balas F, Cauda V, Colilla M, Delgado M, Vallet-Regi M (2008) Studies on MCM-41 mesoporous silica for drug delivery: effect of particle morphology and amine functionalization. *Chem Eng J* 137(1):30–37. <https://doi.org/10.1016/j.cej.2007.07.078>
- McMillan P (1984) Structural studies of silicate glasses and melts-applications and limitations of Raman spectroscopy. *Am Miner* 69(7–8):622–644
- Meena J, Gupta A, Ahuja R et al (2020) Inorganic nanoparticles for natural product delivery: a review. *Environ Chem Lett*. <https://doi.org/10.1007/s10311-020-01061-2>
- Meguid S, Elzaabalawy A (2020) Potential of combating transmission of COVID-19 using novel self-cleaning superhydrophobic surfaces: part I—protection strategies against fomites. *Int J Mech Mater Des* 16(3): 423–431. <https://doi.org/10.1007/s10999-020-09513-x>
- Mehdi YA, Itatahine A, Fizir M, Xiao D, Dramou P, He H (2018) Multifunctional core-shell silica microspheres and their performance in self-carrier decomposition, sustained drug release and fluorescent bioimaging. *J Solid State Chem* 263:148–156. <https://doi.org/10.1016/j.jssc.2018.04.024>
- Mei X, Chen D, Li N, Xu Q, Ge J, Li H, Lu J (2012) Hollow mesoporous silica nanoparticles conjugated with pH-sensitive amphiphilic diblock polymer for controlled drug release. *Microporous Mesoporous Mater* 152:16–24. <https://doi.org/10.1016/j.micromeso.2011.12.015>
- Miller JR, Simon P (2008) Electrochemical capacitors for energy management. *Science Magazine* 321(5889):651–652. <https://doi.org/10.1126/science.1158736>
- Mohanraj K, Kannan S, Barathan S, Sivakumar G (2012) Preparation and characterization of nano SiO<sub>2</sub> from corn cob ash by precipitation method.
- Mokhtar H, Ramlah M, Aida Isma M, Huda N (2016) Characterization on silica from waste sugarcane bagasse for membrane fabrication. *Jurnal Teknologi* 78(5–4):43–47. <https://doi.org/10.11113/jt.v78.8539>
- Moosa AA, Saddam BF (2017) Synthesis and characterization of nano-silica from rice husk with applications to polymer composites. *Am J Mater Sci* 7(6):223–231
- Morimoto H, Minato M, Nakagawa T, Sato M, Kobayashi Y, Gonda K, Takeda M, Ohuchi N, Suzuki N (2011) X-ray imaging of newly-developed gadolinium compound/silica core-shell particles. *J Sol-Gel Sci Technol* 59(3):650. <https://doi.org/10.1007/s10971-011-2540-6>
- Morin-Crini N, Fourmentin M, Fourmentin S, Torri G, Crini GJECL (2019) Synthesis of silica materials containing cyclodextrin and their applications in wastewater treatment. *Environ Chem Lett* 17(2):683–696. <https://doi.org/10.1007/s10311-018-00818-0>
- Mozzi R, Warren B (1969) The structure of vitreous silica. *J Appl Crystallogr* 2(4):164–172. <https://doi.org/10.1107/s0021889869006868>
- Naqvi HJ, Saeed A, Umair A, Shah FH (2011) Precipitated silica from wheat husk. *J Pakistan Instit Chem Eng* 39(1):51–54
- Novak F, Plumeré N, Schetter B, Speiser B, Straub D, Mayer HA, Reginek M, Albert K, Fischer G, Meyer C (2010) Redox-active silica nanoparticles. Part 4. Synthesis, size distribution, and electrochemical adsorption behavior of ferrocene-and (diamine) (diphosphine)-ruthenium (II)-modified Stöber silica colloidal particles. *Journal of Solid State Electrochemistry* 14 (2), 289–303. <https://doi.org/10.1007/s10008-009-0811-8>
- NPMCR (2019) Accessed on 6 March 2019. Available online: [https://agricoop.nic.in/sites/default/files/NPMCR\\_1.pdf](https://agricoop.nic.in/sites/default/files/NPMCR_1.pdf).
- Okoronkwo E, Imoisili P, Olusunle S (2013) Extraction and characterization of amorphous silica from corn cob ash by sol-gel method. *Chem Mater Res* 3(4):68–72
- Okoronkwo EA, Imoisili PE, Olubayode SA, Olusunle SO (2016) Development of silica nanoparticle from corn cob ash. *Adv Nanoparticles* 5(02):135. <https://doi.org/10.4236/anp.2016.52015>
- Oladeji J (2010) Fuel characterization of briquettes produced from corncob and rice husk residues. *Pac J Sci Technol* 11(1):101–106
- Osipov A, Osipova L, Zainullina RJIJoS (2015) Raman spectroscopy and statistical analysis of the silicate species and group connectivity in cesium silicate glass forming system. *Int J Spectroscopy*, 1–15. <https://doi.org/10.1155/2015/572840>
- Ow H, Larson DR, Srivastava M, Baird BA, Webb WW, Wiesner U (2005) Bright and stable core-shell fluorescent silica nanoparticles. *Nano Lett* 5(1):113–117. <https://doi.org/10.1021/nl0482478>
- Owoeye SS, Oji B, Aderiye J (2015) Effect of temperature, time and atmospheric condition on active silica extraction from Corn Cob ash. *Int J Eng Technol Innovat* 2:1–5
- Pandey S, Mewada A, Thakur M, Pillai S, Dharmatti R, Phadke C, Sharon M (2014) Synthesis of mesoporous silica oxide/C-dot complex (meso-SiO<sub>2</sub>/C-dots) using pyrolysed rice husk and its application in bioimaging. *RSC Adv* 4(3):1174–1179. <https://doi.org/10.1039/c3ra45227a>
- Pauling L (1957) Discovery of the elements. ACS Publications, Mary Elvira. <https://doi.org/10.1021/ed034p51.1>
- Peng H, Dong R, Wang S, Zhang Z, Luo M, Bai C, Zhao Q, Li J, Chen L, Xiong H (2013) A pH-responsive nano-carrier with mesoporous silica nanoparticles cores and poly (acrylic acid) shell-layers: fabrication, characterization and properties for

- controlled release of salidroside. *Int J Pharm* 446(1–2):153–159. <https://doi.org/10.1016/j.ijpharm.2013.01.071>
- Pinho SL, Pereira GA, Voisin P, Kassem J, Bouchaud V, Etienne L, Peters JA, Carlos L, Mornet S, Gerales CF (2010) Fine tuning of the relaxometry of  $\gamma$ -Fe<sub>2</sub>O<sub>3</sub>@ SiO<sub>2</sub> nanoparticles by tweaking the silica coating thickness. *ACS Nano* 4(9):5339–5349. <https://doi.org/10.1021/nn101129r>
- Peng Z, Kong LX, Li S-D, Chen Y, Huang MFJCS (2007) Self-assembled natural rubber/silica nanocomposites: its preparation and characterization. *Compos Sci Technol* 67(15–16):3130–3139. <https://doi.org/10.1016/j.compscitech.2007.04.016>
- Pode RJR, Reviews SE (2016) Potential applications of rice husk ash waste from rice husk biomass power plant. *Renew Sustain Energy Rev* 53:1468–1485. <https://doi.org/10.1016/j.rser.2015.09.051>
- Prabha S, Durgalakshmi D, Aruna P, Ganesan SJV (2019) Influence of the parameters in the preparation of silica nanoparticles from biomass and chemical silica precursors towards bioimaging application. *Vacuum* 160:181–188. <https://doi.org/10.1016/j.vacuum.2018.11.030>
- Qi D, Lin C, Zhao H, Liu H, Lü T (2017) Size regulation and prediction of the SiO<sub>2</sub> nanoparticles prepared via Stöber process. *J Dispersion Sci Technol* 38(1):70–74. <https://doi.org/10.1080/01932691.2016.1143373>
- Qin X, Yin Y, Yu H, Guo W, Pei M (2016) A novel signal amplification strategy of an electrochemical aptasensor for kanamycin, based on thionine functionalized graphene and hierarchical nanoporous PtCu. *Biosens Bioelectron* 77:752–758. <https://doi.org/10.1016/j.bios.2015.10.050>
- Rahman NA, Widhiana I, Juliastuti SR, Setyawan H (2015) Synthesis of mesoporous silica with controlled pore structure from bagasse ash as a silica source. *Colloids Surf A* 476:1–7. <https://doi.org/10.1016/j.colsurfa.2015.03.018>
- Rahmat N, Sabali MA, Sandu AV, Sahiron N, Sandu IG (2016) Study of calcination temperature and concentration of NaOH effect on crystallinity of silica from sugarcane Bagasse Ash (SCBA). *Rev Chim* 67(9):1872–1875
- Ramadhansyah P, Salwa M, Mahyun A, Bakar BA, Johari MM, Norazman CCJPE (2012) Properties of concrete containing rice husk ash under sodium chloride subjected to wetting and drying. *Proc Eng* 50:305–313. <https://doi.org/10.1016/j.proeng.2012.10.035>
- Rao KS, El-Hami K, Kodaki T, Matsushige K, Makino K (2005) A novel method for synthesis of silica nanoparticles. *J Colloid Interface Sci* 289(1):125–131. <https://doi.org/10.1016/j.jcis.2005.02.019>
- Rastogi A, Tripathi DK, Yadav S, Chauhan DK, Živčák M, Ghorbanpour M, El-Sheery NI, Brestic MJB (2019) Application of silicon nanoparticles in agriculture. *Biotech* 9(3), 90. <https://doi.org/10.1007/s13205-019-1626-7>
- Razo DAS, Pallavidino L, Garrone E, Geobaldo F, Descrovi E, Chiodoni A, Giorgis F (2008) A version of Stöber synthesis enabling the facile prediction of silica nanospheres size for the fabrication of opal photonic crystals. *J Nanopart Res* 10(7):1225–1229. <https://doi.org/10.1007/s11051-008-9373-4>
- Rezaei S, Manoucheri I, Moradian R, Pourabbas BJCEJ (2014) One-step chemical vapor deposition and modification of silica nanoparticles at the lowest possible temperature and superhydrophobic surface fabrication. *J Nanotechnol* 252:11–16. <https://doi.org/10.1016/j.cej.2014.04.100>
- Riaz S, Ashraf M, Hussain T, Hussain MTJC (2019) Modification of silica nanoparticles to develop highly durable superhydrophobic and antibacterial cotton fabrics. *Cellulose* 26(8):5159–5175. <https://doi.org/10.1007/s10570-019-02440-x>
- Rodrigues A, Emeje M (2012) Recent applications of starch derivatives in nanodrug delivery. *Carbohydr Polym* 87(2):987–994. <https://doi.org/10.1016/j.carbpol.2011.09.044>
- Rossi LM, Shi L, Quina FH, Rosenzweig Z (2005) Stöber synthesis of monodispersed luminescent silica nanoparticles for bioanalytical assays. *Langmuir* 21(10):4277–4280. <https://doi.org/10.1021/la0504098>
- Saei AA, Dolatabadi JEN, Najafi-Marandi P, Abhari A, de la Guardia M (2013) Electrochemical biosensors for glucose based on metal nanoparticles. *Trends Anal Chem* 42:216–227. <https://doi.org/10.1016/j.trac.2012.09.011>
- Sahoo SK, Labhasetwar V (2003) Nanotech approaches to drug delivery and imaging. *Drug Discovery Today* 8(24):1112–1120. [https://doi.org/10.1016/s1359-6446\(03\)02903-9](https://doi.org/10.1016/s1359-6446(03)02903-9)
- Saito G, Sasaki H, Takahashi H, Sakaguchi NJN (2018) Solution-plasma-mediated synthesis of Si nanoparticles for anode material of lithium-ion batteries. *Nanomater Nanotechnol* 8(5):286. <https://doi.org/10.3390/nano8050286>
- Salh R (2011) 'Defect related luminescence in silicon dioxide network: a review.' (InTech Rijeka) [doi.org/https://doi.org/10.5772/22607](https://doi.org/10.5772/22607)
- Santra S, Yang H, Dutta D, Stanley JT, Holloway PH, Tan W, Moudgil BM, Mericle RA (2004) TAT conjugated, FITC doped silica nanoparticles for bioimaging applications. *Chem Commun* 24:2810–2811. <https://doi.org/10.1039/b411916a>
- Satvekar RK, Pawar SH (2018) Multienzymatic Cholesterol Nanobiosensor Using Core-Shell Nanoparticles Incorporated Silica Nanocomposite. *J Med Biol Eng*, 1–9. <https://doi.org/10.1007/s40846-017-0345-y>
- Saxena R, Adhikari D, Goyal H (2009) Biomass-based energy fuel through biochemical routes: a review. *Renew Sustain Energy Rev* 13(1):167–178. <https://doi.org/10.1016/j.rser.2007.07.011>
- Shariff A, Aziz NSM, Ismail NI, Abdullah N (2016) Corn cob as a potential feedstock for slow pyrolysis of biomass. *J Phys Sci* 27(2):123. <https://doi.org/10.21315/jps2016.27.2.9>
- Shim J, Velmurugan P, Oh B-T (2015) Extraction and physical characterization of amorphous silica made from corn cob ash at variable pH conditions via sol gel processing. *J Ind Eng Chem* 30:249–253. <https://doi.org/10.1016/j.jiec.2015.05.029>
- Shyam M (2002) Agro-residue-based renewable energy technologies for rural development. *Energy Sustain Dev* 6(2):37–42. [https://doi.org/10.1016/s0973-0826\(08\)60311-7](https://doi.org/10.1016/s0973-0826(08)60311-7)
- Silva GA (2004) Introduction to nanotechnology and its applications to medicine. *Surg Neurol* 61(3):216–220. <https://doi.org/10.1016/j.surneu.2003.09.036>
- Silviana S, Bayu WJ (2018) Silicon conversion from bamboo leaf silica by magnesiothermic reduction for development of Li-ion battery anode, MATEC Web of Conferences'.2018 (EDP Sciences) [doi.org/https://doi.org/10.1051/mateconf/201815605021](https://doi.org/10.1051/mateconf/201815605021)
- Simon P, Gogotsi Y (2010) Materials for electrochemical capacitors. In: *Nanoscience and technology: a collection of reviews from nature journals*. World Scientific, Singapore, pp 320–329 [https://doi.org/10.1142/9789814287005\\_0033](https://doi.org/10.1142/9789814287005_0033)
- Singh L, Agarwal S, Bhattacharyya S, Sharma U, Ahalawat S (2011) Preparation of silica nanoparticles and its beneficial role in cementitious materials. *Nanomater Nanotechnol* 1(1):44–51. <https://doi.org/10.5772/50950>
- Singh LP, Bhattacharyya SK, Kumar R, Mishra G, Sharma U, Singh G, Ahalawat S (2014) Sol-Gel processing of silica nanoparticles and their applications. *Adv Coll Interface Sci* 214:17–37. <https://doi.org/10.1016/j.cis.2014.10.007>
- Singh N, Karambelkar A, Gu L, Lin K, Miller JS, Chen CS, Sailor MJ, Bhatia SN (2011) Bioresponsive mesoporous silica nanoparticles for triggered drug release. *J Am Chem Soc* 133(49):19582–19585. <https://doi.org/10.1021/ja206998x>
- Singh RK, Patel KD, Kim J-J, Kim T-H, Kim J-H, Shin US, Lee E-J, Knowles JC, Kim H-W (2014) Multifunctional hybrid nanocarrier: magnetic CNTs ensheathed with mesoporous silica for drug delivery and imaging system. *ACS Appl Mater Interfaces* 6(4):2201–2208. <https://doi.org/10.1021/am4056936>

- Singh SKL, All Jawald S (2013) Utilization of sugarcane bagasse ash (SCBA) as pozzolanic material in concrete. A review, IJBSTR
- Slowing II, Trewyn BG, Giri S, Lin VY (2007) Mesoporous silica nanoparticles for drug delivery and biosensing applications. *Adv Func Mater* 17(8):1225–1236. <https://doi.org/10.1002/adfm.200601191>
- Song J-T, Yang X-Q, Zhang X-S, Yan D-M, Yao M-H, Qin M-Y, Zhao Y-D (2015) Composite silica coated gold nanosphere and quantum dots nanoparticles for X-ray CT and fluorescence bimodal imaging. *Dalton Trans* 44(25):11314–11320. <https://doi.org/10.1039/c5dt01286d>
- Song Q, Peng M, Wang L, He D, Ouyang J (2016) A fluorescent aptasensor for amplified label-free detection of adenosine triphosphate based on core-shell Ag@ SiO<sub>2</sub> nanoparticles. *Biosens Bioelectron* 77:237–241. <https://doi.org/10.1016/j.bios.2015.09.008>
- Sounderya N, Zhang Y (2008) Use of core/shell structured nanoparticles for biomedical applications. *Recent Patents Biomed Eng* 1(1):34–42. <https://doi.org/10.2174/1874764710801010034>
- Shen Y, Zhao P, Shao Q (2014) Porous silica and carbon derived materials from rice husk pyrolysis char. *Microporous Mesoporous Mater* 188:46–76. <https://doi.org/10.1016/j.micro-meso.2014.01.005>
- Shimura N, Ogawa M (2007) Preparation of surfactant templated nanoporous silica spherical particles by the Stöber method. Effect of solvent composition on the particle size. *J Mater Sci* 42(14):5299–5306
- Srinivasan K, Subramanian K, Rajasekar A, Murugan K, Benelli G, Dinakaran K (2017) A sensitive optical sensor based on DNA-labelled Si@SiO<sub>2</sub> core-shell nanoparticle for the detection of Hg<sup>2+</sup> ions in environmental water samples. *Bull Mater Sci* 40(7):1455–1462. <https://doi.org/10.1007/s12034-017-1486-x>
- Stanley RA, Nesaraj AS (2014) Effect of surfactants on the wet chemical synthesis of silica nanoparticles. *Int J Appl Sci Eng* 12:9–21. [https://doi.org/10.6703/IJASE.2014.12\(1\).9](https://doi.org/10.6703/IJASE.2014.12(1).9)
- Stefanakis D, Ghanotakis D (2014) Synthesis and characterization of nanoparticles, consisting of a gadolinium paramagnetic core and a mesoporous silica shell, for controlled delivery of hydrophobic drugs. *J Nanopart Res* 16(1):2211. <https://doi.org/10.1007/s11051-013-2211-3>
- Stöber W, Fink A, Bohn E (1968) Controlled growth of monodisperse silica spheres in the micron size range. *J Colloid Interface Sci* 26(1):62–69. [https://doi.org/10.1016/0021-9797\(68\)90272-5](https://doi.org/10.1016/0021-9797(68)90272-5)
- Sumathi R, Thenmozhi R (2016) Preparation of spherical silica nanoparticles by Sol-Gel method, II. In: International conference on systems, science, control, communication, engineering and technology
- Suzuki K, Ikari K, Imai H (2004) Synthesis of silica nanoparticles having a well-ordered mesostructure using a double surfactant system. *J Am Chem Soc* 126(2):462–463. <https://doi.org/10.1021/ja038250d>
- Tadanaga K, Morita K, Mori K, Tatsumisago M (2013) Synthesis of monodispersed silica nanoparticles with high concentration by the Stöber process. *J Sol-Gel Sci Technol* 68(2):341–345. <https://doi.org/10.1007/s10971-013-3175-6>
- Tan SY, Teh C, Ang CY, Li M, Li P, Korzh V, Zhao Y (2017) Responsive mesoporous silica nanoparticles for sensing of hydrogen peroxide and simultaneous treatment toward heart failure. *Nanoscale* 9(6):2253–2261. <https://doi.org/10.1039/c6nr08869d>
- Tang J, Slowing II, Huang Y, Trewyn BG, Hu J, Liu H, Lin VS-Y (2011) Poly (lactic acid)-coated mesoporous silica nanosphere for controlled release of venlafaxine. *J Colloid Interface Sci* 360(2):488–496. <https://doi.org/10.1016/j.jcis.2011.05.027>
- Tang L, Cheng J (2013) Nonporous silica nanoparticles for nanomedicine application. *Nano Today* 8(3):290–312. <https://doi.org/10.1016/j.nantod.2013.04.007>
- Thomas M, Slipper I, Walunj A, Jain A, Favretto M, Kallinteri P, Douroumis D (2010) Inclusion of poorly soluble drugs in highly ordered mesoporous silica nanoparticles. *Int J Pharm* 387(1–2):272–277. <https://doi.org/10.1016/j.ijpharm.2009.12.023>
- Todkar B, Deorukhar O, Deshmukh S (2016) Extraction of silica from rice husk. *Int J Eng Res Dev* 12:69–74
- Trewyn BG, Slowing II, Giri S, Chen H-T, Lin VS-Y (2007) Synthesis and functionalization of a mesoporous silica nanoparticle based on the sol-gel process and applications in controlled release. *Acc Chem Res* 40(9):846–853. <https://doi.org/10.1021/ar600032u>
- Tsai W, Chang C, Wang S, Chang C, Chien S, Sun H (2001) Cleaner production of carbon adsorbents by utilizing agricultural waste corn cob. *Resour Conserv Recycl* 32(1):43–53. [https://doi.org/10.1016/s0921-3449\(00\)00093-8](https://doi.org/10.1016/s0921-3449(00)00093-8)
- Tyagi V, Pandit S, Sharma A, Gupta RK (2017) Extraction and characterization of silica from rice husk for use in food industries. *Extraction* 2(4)
- Tzankov B, Yoncheva K, Lambov N (2014) Mesoporous silica nanoparticles as drug carriers. *Pharmacia* 61(1):27–37
- Vallet-Regí M, Colilla M, González B (2011) Medical applications of organic-inorganic hybrid materials within the field of silica-based bioceramics. *Chem Soc Rev* 40(2):596–607. <https://doi.org/10.1039/c0cs00025f>
- Vallet-Regí M, Balas F, Arcos D (2007) Mesoporous materials for drug delivery. *Angew Chem Int Ed* 46(40):7548–7558
- Vansant EF, Van Der Voort P, Vrancken KC (1995) Characterization and chemical modification of the silica surface. Elsevier, Amsterdam. [https://doi.org/10.1016/s0167-2991\(06\)81511-9](https://doi.org/10.1016/s0167-2991(06)81511-9)
- Vazquez NI, Gonzalez Z, Ferrari B, Castro Y (2017) Synthesis of mesoporous silica nanoparticles by sol-gel as nanocontainer for future drug delivery applications. *Boletín de la Sociedad Española de Cerámica y Vidrio* 56(3):139–145. <https://doi.org/10.1016/j.bsecev.2017.03.002>
- Velmurugan P, Shim J, Lee K-J, Cho M, Lim S-S, Seo S-K, Cho K-M, Bang K-S, Oh B-T (2015) Extraction, characterization, and catalytic potential of amorphous silica from corn cobs by sol-gel method. *J Ind Eng Chem* 29:298–303. <https://doi.org/10.1016/j.jiec.2015.04.009>
- Verma MLJECL (2017) Nanobiotechnology advances in enzymatic biosensors for the agri-food industry. *Environ Chem Lett* 15(4):555–560. <https://doi.org/10.1007/s10311-017-0640-4>
- Viarbitskaya S, Ryderfors L, Mikaelsson T, Mukhtar E, Johansson LB-Å (2011) Luminescence enhancement from silica-coated gold nanoparticle agglomerates following multi-photon excitation. *J Fluores* 21(1):257–264. <https://doi.org/10.1007/s10895-010-0713-2>
- Vijayan R, Kumar GS, Karunakaran G, Surumbarkuzhali N, Prabhu S, Ramesh R (2020) Microwave combustion synthesis of tin oxide-decorated silica nanostructure using rice husk template for supercapacitor applications. *J Mater Sci: Mater Electron*, 1–8. <https://doi.org/10.1007/s10854-020-03142-y>
- Viswanathan S, Kovacs Z, Green KN, Ratnakar SJ, Sherry AD (2010) Alternatives to gadolinium-based metal chelates for magnetic resonance imaging. *Chem Rev* 110(5):2960–3018. <https://doi.org/10.1021/cr900284a>
- Vivero-Escoto JL, Huang Y-T (2011) Inorganic-organic hybrid nanomaterials for therapeutic and diagnostic imaging applications. *Int J Mol Sci* 12(6):3888–3927. <https://doi.org/10.3390/ijms12063888>
- Vu KB, Bach LG, Van Tran T, Thuong NT, Giang H, Bui QTP, Ngo STJCLP (2019) Gold@ silica catalyst: porosity of silica shells



- switches catalytic reactions. *Chem Phys Lett* 728:80–86. <https://doi.org/10.1016/j.cplett.2019.04.082>
- Waddell WH (2000) Silica, amorphous. *Kirk-Othmer Encycl Chem Technol*. <https://doi.org/10.1002/0471238961.0113151823010404.a01>
- Wan MM, Yang JY, Qiu Y, Zhou Y, Guan CX, Hou Q, Lin WG, Zhu JH (2012) Sustained release of heparin on enlarged-pore and functionalized MCM-41. *ACS Appl Mater Interfaces* 4(8):4113–4122. <https://doi.org/10.1021/am300878z>
- Wang X-D, Shen Z-X, Sang T, Cheng X-B, Li M-F, Chen L-Y, Wang Z-S (2010) Preparation of spherical silica particles by Stöber process with high concentration of tetra-ethyl-orthosilicate. *J Colloid Interface Sci* 341(1):23–29. <https://doi.org/10.1016/j.jcis.2009.09.018>
- Wassie AB, Srivastava VC (2017) Synthesis and characterization of Nano-Silica from Teff Straw. *J Nano Res (Trans Tech Publ)*. <https://doi.org/10.4028/www.scientific.net/jnanor.46.64>
- Winter M, Brodd RJ (2004) What are batteries, fuel cells, and supercapacitors? *Chem Rev ACS Publ* 104(10):4245–4270. <https://doi.org/10.1021/cr020730k>
- Wu L, Zhou Y, Nie W, Song L, Chen P (2015) Synthesis of highly monodispersed teardrop-shaped core-shell SiO<sub>2</sub>/TiO<sub>2</sub> nanoparticles and their photocatalytic activities. *Appl Surf Sci* 351:320–326. <https://doi.org/10.1016/j.apsusc.2015.05.152>
- Wu X, Wang Z, Zhu D, Zong S, Yang L, Zhong Y, Cui Y (2013) pH and thermo dual-stimuli-responsive drug carrier based on mesoporous silica nanoparticles encapsulated in a copolymer-lipid bilayer. *ACS Appl Mater Interfaces* 5(21):10895–10903. <https://doi.org/10.1021/am403092m>
- Wu S-H, Mou C-Y, Lin H-P (2013) Synthesis of mesoporous silica nanoparticles. *Chem Soc Rev* 42:3862–3875. <https://doi.org/10.1039/C3CS35405A>
- Yanagisawa T, Shimizu T, Kuroda K, Kato C (1990) The preparation of alkyltriethylammonium-kaneinite complexes and their conversion to microporous materials. *Bull Chem Soc Jpn* 63(4):988–992. <https://doi.org/10.1246/bcsj.63.988>
- Yermekova Z, Mansurov Z, Mukasyan AJJoS-PH-TS (2010) Combustion synthesis of silicon nanopowders. *Int J Self Propag High Temp Synth* 19(2):94–101. <https://doi.org/10.3103/s1061386210020032>
- Yogeswaran U, Chen S-M (2008) A review on the electrochemical sensors and biosensors composed of nanowires as sensing material. *Sensors* 8(1):290–313. <https://doi.org/10.3390/s8010290>
- You B, Yang J, Sun Y, Su Q (2011) Easy synthesis of hollow core, bimodal mesoporous shell carbon nanospheres and their application in supercapacitor. *Chem Commun* 47(45):12364–12366. <https://doi.org/10.1039/c1cc15348j>
- Yu C-H, Tam K, Tsang ES (2008) Chemical methods for preparation of nanoparticles in solution. *Handbook Metal Phys* 5:113–141
- Yu K, Guo Y, Ding X, Zhao J, Wang Z (2005) Synthesis of silica nanocubes by sol-gel method. *Mater Lett* 59(29–30):4013–4015. <https://doi.org/10.1016/j.matlet.2005.07.055>
- Yu T, Malugin A, Ghandehari H (2011) Impact of silica nanoparticle design on cellular toxicity and hemolytic activity. *ACS Nano* 5(7):5717–5728. <https://doi.org/10.1021/nn2013904>
- Yuan J, Zhou S, Gu G, Wu L (2005) Encapsulation of organic pigment particles with silica via sol-gel process. *J Sol-Gel Sci Technol* 36(3):265–274. <https://doi.org/10.1007/s10971-005-4063-5>
- Yuvakkumar R, Elango V, Rajendran V, Kannan N (2014) High-purity nano silica powder from rice husk using a simple chemical method. *J Exp Nanosci* 9(3):272–281. <https://doi.org/10.1080/17458080.2012.656709>
- Zainala NA, Shukor SRA, Wabb HAA, Razakb K (2013) Study on the effect of synthesis parameters of silica nanoparticles entrapped with rifampicin. *Chem Eng Trans* 32:2245–2250
- Zakaria J, Shukor SRA, Zainal NA, Abdul K Production of silica nanoparticles entrapped with Rifampicin: effect of surfactant, stirring rate and water content.
- Zeng D, Zhang H, Wang B, Sang K, Yang J (2015) Effect of ammonia concentration on silica spheres morphology and solution hydroxyl concentration in Stober process. *J Nanosci Nanotechnol* 15(9):7407–7411. <https://doi.org/10.1166/jnn.2015.10595>
- Zemnukhova L, Kharchenko U, Beleneva I (2015) Biomass derived silica containing products for removal of microorganisms from water. *Int J Environ Sci Technol* 12(5):1495–1502. <https://doi.org/10.1007/s13762-014-0529-8>
- Zhang Y, Gao F, Wanjala B, Li Z, Cernigliaro G, Gu ZJACBE (2016) High efficiency reductive degradation of a wide range of azo dyes by SiO<sub>2</sub>-Co core-shell nanoparticles. *Appl Catal B* 199:504–513. <https://doi.org/10.1016/j.apcatb.2016.06.030>
- Zhao Y, Vivero-Escoto JL, Slowing II, Trewyn BG, Lin VS (2010) Capped mesoporous silica nanoparticles as stimuli-responsive controlled release systems for intracellular drug/gene delivery. *Expert Opin Drug Delivery* 7(9):1013–1029. <https://doi.org/10.1517/17425247.2010.498816>
- Zhou Z, Zhang C, Qian Q, Ma J, Huang P, Pan L, Gao G, Fu H, Fu S, Song H (2013) Folic acid-conjugated silica capped gold nanoclusters for targeted fluorescence/X-ray computed tomography imaging. *J Nanobiotechnol* 11(1):17. <https://doi.org/10.1186/1477-3155-11-17>
- Zhu T, Hu Y, Yang K, Dong N, Yu M, Jiang N (2018) A novel SERS nanoprobe based on the use of core-shell nanoparticles with embedded reporter molecule to detect *E. coli* O157: H7 with high sensitivity. *Microchimica Acta* 185(1), 30. <https://doi.org/10.1007/s00604-017-2573-9>

**Publisher's Note** Springer Nature remains neutral with regard to jurisdictional claims in published maps and institutional affiliations.